UNIVERSIDAD DE INVESTIGACIÓN DE TECNOLOGÍA EXPERIMENTAL YACHAY

Escuela de Ciencias Biológicas e Ingeniería

TÍTULO: Artificial Intelligence to diagnose low back pain using motion captures.

Trabajo de integración curricular presentado como requisito para la obtención del título de Ingeniero Biomédico.

Autor:

Loján Cueva Alejandro Bolívar

Tutor:

PhD. Villalba Meneses Gandhi Fernando

Co-tutor:

PhD. Tirado Espín Christian Andrés

Urcuquí, octubre 2023

Autoría

Yo, **ALEJANDRO BOLÍVAR LOJÁN CUEVA**, con número de cédula de identidad CI: 1724400351, declaro que las ideas, juicios, valoraciones, interpretaciones, consultas bibliográficas, definiciones y conceptualizaciones expuestas en el presente trabajo; así cómo, los procedimientos y herramientas utilizadas en la investigación, son de absoluta responsabilidad de el/la autora (a) del trabajo de integración curricular. Así mismo, me acojo a los reglamentos internos de la Universidad de Investigación de Tecnología Experimental Yachay.

Urcuquí, octubre 2023.

Firmado electrónicamente por:
ALEJANDRO BOLIVAR LOJAN CUEVA

Alejandro Bolívar Loján Cueva

CI: 1724400351

Autorización de publicación

Yo, **ALEJANDRO BOLÍVAR LOJÁN CUEVA**, con número de cédula de identidad CI: 1724400351, cedo a la Universidad de Investigación de Tecnología Experimental Yachay, los derechos de publicación de la presente obra, sin que deba haber un reconocimiento económico por este concepto. Declaro además que el texto del presente trabajo de titulación no podrá ser cedido a ninguna empresa editorial para su publicación u otros fines, sin contar previamente con la autorización escrita de la Universidad.

Asimismo, autorizo a la Universidad que realice la digitalización y publicación de este trabajo de integración curricular en el repositorio virtual, de conformidad a lo dispuesto en el Art. 144 de la Ley Orgánica de Educación Superior

Urcuquí, octubre 2023.

Firmado electrónicamente por:
ALEJANDRO BOLIVAR LOJAN CUEVA

Alejandro Bolívar Loján Cueva

CI: 1724400351

Dedicatoria

Dedico este trabajo a mis padres Bolívar y Cecilia, quienes han estado a mi lado en cada etapa de mi vida brindándome apoyo. Gracias por su amor incondicional, paciencia y sacrificio, por creer en mí y por guiarme en los momentos de incertidumbre.

A mi hermana Pamela, por ser mi confidente y por estar a mi lado siempre. Gracias por compartir mis sueños y por alentarme a ser una mejor persona.

A Karol, mi compañera de vida durante mi carrera universitaria. Gracias por estar presente en cada paso de mi camino, por las risas y lágrimas que juntos compartimos. Gracias por ser una parte importante de mi vida.

Y a Sebastián, Martina, Naomi, Nathalia, Luis y Christian amigos que se convirtieron en la familia que elegí, siempre los llevaré en el corazón. Con ustedes compartí una de las mejores etapas de mi vida.

Este logro no habría sido posible sin el amor, la paciencia y el apoyo de todos ustedes. Les dedico este trabajo con todo mi corazón y les agradezco por ser parte de mi vida y por ayudarme a llegar hasta aquí. Espero poder seguir contando con su apoyo en el futuro.

- Alejandro Bolívar Loján Cueva

Agradecimientos

En primer lugar, mis profundos agradecimientos a mi tutor de tesis Fernando Villalba por su dedicación y entrega durante todo el proceso de elaboración de este proyecto de titulación. Gracias a él pude contar con todas las herramientas necesarias para poner en alto mi carrera como ingeniero biomédico. Siempre estuvo disponible para aclarar mis dudas, aconsejarme y guiarme en cada etapa del proyecto. Su actitud positiva y perseverante ante los problemas fueron una fuente de inspiración constante para mí.

También quiero agradecer al Centro Fisiomedics por permitirnos trabajar con decenas de pacientes durante la realización de este proyecto. Siempre brindando una atención amable, cordial y su apoyo desinteresado.

De la misma forma, quiero agradecer a Emilio Paspuél y Darwin Quinteros por su liderazgo y labor logistica que fueron fundamentales para sacar adelante este proyecto de tesis. Finalmente a Elaine Herrera por su valioso apoyo y amistad durante estos años de carrera.

- Alejandro Bolivar Loján Cueva

Resumen

La lumbalgia es una afección musculoesquelética común y la principal causa de ausentismo laboral, sin embargo, en la mayoría de los casos no se identifica el origen del dolor nociceptivo y a pesar de ello se administra fisioterapia. Una de las valoraciones más importantes para la evaluación del dolor lumbar es el análisis de la rango de movimiento (ROM) que consiste en calcular la diferencia de ángulos desde la posición de inicial hasta el punto de máximo alcance en múltiples ejercicios axiales y este carece de precision ya que se realiza con cintas métricas. Este proyecto de tesis se basa en la aplicación de técnicas de captura de movimiento (MoCap) con unidades de sensores inerciales para obtener medidas espacio-temporales precisas con el objetivo de evaluar ejercicios de un grupo de pacientes sanos y otro con pacientes diagnosticado con lumbalgia de la provincia de Imbabura, Ecuador con el fin de automatizar la clasificación de rangos normales y patológicos de movimiento, utilizando siete algoritmos de aprendizaje automático (Regresión logística, SVM, K-nearest neighbours, árbol de decisión, Random forest, Gradient boosting algorthm y Multilayer perceptron) para evaluar y comparar las métricas de cada modelor. Todas las técnicas de aprendizaje automático obtuvieron una precisión superior al 80% y tres modelos obtuvieron una precisión superior al 90% (Support Vector Machines, Random forest, Multilayer perceptron), concluyendo que el mejor algorithmo es SVM. Los resultados obtenidos comparten un comportamiento similar en comparación con trabajos relacionados.

Palabras Clave:
MoCap, Clasificación, Rango de movimiento, Machine Learning, Lumbalgia.

Abstract

Low back pain (LBP) is a highly common musculoskeletal condition and the leading cause of work absenteeism, yet in most cases the source of nociceptive pain is rarely identified and physical therapy duration is administered regardless. One of the most important evaluation assessments for LBP is range of motion analysis (ROM) that consists of calculating the difference in angles between the standing position and the maximum reaching point in multiple axial exercises, at present ROM is performed with taping measure lacking precision. This graduation project is based in the application of motion capture (MoCap) techniques with inertial sensor units for precise spatiotemporal measures to assess ROM exercises from healthy and clinically diagnosed patients with LBP from Imbabura, Ecuador in order to automate classification of normal or pathological ranges of movement using seven machine learning algorithms (Logistic regression, SVM, K-nearest neighbours, Decision tree, Random forest, Gradient boosting algorithm and Multilayer perceptron) to evaluate and compare the resulting metrics. All machine learning techniques obtained accuracy above 80% and three models obtained >90% accuracy (Support Vector Machines, Random forest, Multilayer perceptron), concluding SVM is the best performing algorithm. Obtained results share similar behavior compared to related works.

Keywords:
MoCap, Classification, Range of movement, Machine Learning, Low back pain.

Contents

List of Figures

List of Tables

List of Equations

Chapter 1

Introduction

1.1 Problem Statement

Low back pain (LBP) is a highly common musculoskeletal condition, related to affection in spinal structures, ligament injuries or natural aging factors [Hoy et al., 2010, PAHO, 2019]. Millions of dollars are spent in the healthcare system and the cost in work incapacitation increases every year worldwide [Grabois, 2005]. In Ecuador the incidence rates are steadily increasing [Fuseau et al., 2022]. Studies suggest that low back pain originates due to musculoskeletal injuries, age-related degeneration, spinal stenosis and disc herniation. Standard diagnostic practices include physical examination and imaging methods; however, diagnosis can be a aggravating process for patients with nonspecific low back pain, nonetheless the origin of the pathology is uncommonly identified before treatment.

Motion capture (MoCap) is the process of acquiring information about live subjects in motion, standard methods rely on optical, magnetic and even sonic techniques in order to quantify kinematic and motion information. The use of wearable devices with integrated sensors, such as the inertial sensor provide new techniques for the analysis of musculoskeletal diseases. The present work seeks to evaluate the performance of different ML classification algorithms in differentiating pathological subjects from healthy individuals using MoCap data acquired from patients from Imbabura - Ecuador with the Move Human (MH) motion capture system and generate a predictive model with machine learning techniques and provide a tool to improve LBP detection and personalized treatment.

1.2 Thesis overview

This project is divided as follows. Chapter 1: Introduction, establish the importance of the problematic setting background information and objectives of the investigation. Chapter 2, Theoretical framework, comprehends a resume of bibliographical information related to Low back pain and the principles behind the research question and hypothesis stated. Chapter 3: Methodology, is focused in explaining and justifying the procedures and principles to carry out the investigation from data acquisition, feature extraction and machine learning (ML) model testing and evaluation. Chapter 4: Results, presents the outcomes achieved of the seven ML model testing using descriptive statistical analysis followed by Chapter 5: Discussion, where results are thoroughly analyzed to identify possible factors influencing the obtained performance as well as establish the limits of the project. In Chapter 6: Conclusions, a brief description of the research findings is provided in order to establish an answer to the research question and description of future research prospects on how to overcome limitations and improve expected results.

1.3 Hypothesis

Machine learning algorithms can be used to accurately classify healthy and pathological individuals, evaluating significant changes in range of motion using motion capture techniques to enhance screening process of low back pain therapy.

1.4 Objectives

1.4.1 General Objective

Apply and compare different machine learning techniques in clinical data acquired from healthy and pathological patients using MH motion sensors to provide a prognosis tool for medical personnel to determinate whether a patient requires more treatment or not by predicting outcomes with different machine learning classifiers.

1.4.2 Specific Objectives

- Acquire relevant clinical data of healthy and pathological patients diagnosed with LBP with motion capture sensors to assess the active range of motion (ROM) with exercises (Flexo-Extension, Rotation and Lateriztion) to evaluate multi axial move- ment.
- Data base optimization and parameter adjustment to enhance performance and avoidover-parametrization of machine learning models.
- Test and train seven different machine learning classification models in the obtained data base (Logistic regression, SVM, K-nearest neighbours, Decision tree, Random forest, Gradient boosting algorithm and Multilayer perceptron).
- Evaluate and compare the results obtained to determinate the best performance in classification models using accuracy, precision, specificity, F-measure and error.

Chapter 2

Theoretical Framework

2.1 Low back pain, a general description

Low back pain (LBP) can be defined as a group of symptoms associated with physical distress focused around the lower spinal cord area. Experimental research suggests LBP can originate from injuries in the spinal cord and its surrounding structures, the other mainly cause is age-related disk degeneration. [Deyo and Weinstein, 2001]. According to Deyo, et al. it is expected that two thirds of the population will experience LBP in their lifetime [Deyo and Weinstein, 2001].

LBP is the leading cause of work absenteeism and often it is hard to identify the source of nociceptive pain given the complex factor combination (musculoskeletal, enviromenta, emotional, infections, etc. [Patrick et al., 2014]) associated to the disease [Hartvigsen et al., 2018].

Since LBP is a condition that affects the last segment of the spinal column and oftentimes pain and discomfort can irradiate one or both of the lower limbs. regarding the duration of the pathology LBP can be classified as: acute (lasting fewer than 12 weeks), chronic (lasting more than 12 weeks) and recurrent (for patients with repetitive episodes) other authors use the sub-acute classification for symptoms lasting between 6 to 12 weeks [Carpio et al., 2018]. Patients prolonged episodes of acute LBP have an elevated risk of transition from acute to chronic pain [Patrick et al., 2014].

Epidemiology: incidence and prevalence factors

According to the Pan American Health Organization (PAHO) Epidemiology is defined as quantitative study of the frequency distribution of a pathology for control [PAHO, 2019], bibliographical information of the pathology is not uniform and can even be contradictory [Manchikanti, 2000], but some studies suggest that LBP arises from musculoskeletal injuries, age degeneration, spinal stenosis and disk herniation [Deyo and Weinstein, 2001], but many incidence factors have been linked to LBP: age, sex, geographical location, type of work, genetics, morphological condition, social strata and daily habits [Manchikanti, 2000]. Age is the most important incidence factor, the risk of LBP increases with age. Educational level is also related by indirectly prolonging the duration of the pathology, low economic status has been observed to have a tendency of higher risk of LBP and prolonged episodes. Negative psychological factors such as stress, depression and anxiety are associated to elevated risk of LBP [Patrick et al., 2014]. It was found that LBP is one of the leading cause of physician visits every year, apart from the previously mentioned factors it was found that sedentary patients with mild work activities sitting for extended periods (longer than 6 hours represented a higher risk factor for LBP incidence [Ordoñez-Hinojos et al., 2012].

According to Ballina et al. around 84% of the general population will experience LPB in their lifetime, 90% has probability of remitting episodes of LBP with persistent symptoms after apparent relief periods. Only 10% of cases will be remain for more than 12 weeks transcending from acute to chronic episodes. [Ballina et al., 2000]

National and international impact

Given the high incidence and prevalence factors LBP is considered relevant musculoskeletal condition affecting the economy worldwide for two main reasons: loss of work days due to physical incapacitation of global workers and the annually increasing physician visit rate increase. It has been determined the incidence rate is directly proportional to the age of patients increasing constantly until the age of 65 years old [Hoy et al., 2010] leading to life quality limitations and economic impact due to productivity loss and clinical expenses [Katz, 2004]. According to research carried out by Grabois et al. only in the United States LBP in 2005 around 10 million Americans were disabled by pain related to LBP

and 250 million work days were lost each year in addition to millions of dollars spent in physician visits [Grabois, 2005] hence the importance of this problematic for clinicians, public health systems and healthcare resources [Manchikanti, 2000]. Additionally, LBP is a main factor in activity restriction and absence from work worldwide, resulting in a vast economic distress for families, general population and the industry. The increasing health care costs associated to low back pain estimates a loss of 26.3 billion dollars by the early 2000s [Patrick et al., 2014].

In other countries such as Spain around the 0.6% of the gross domestic product (GDP) is lost in sanitary and work related to LBP according to a recent study about herniated disc in the lumbar region in 75 subjects, it is suggested that epidemiological factors need to be evaluated for prevention and control of LBP cases, resulting in significant risk factor for low economical groups [Leac et al., 2022].

The problematic is aggravating for Latino American countries, in Mexico it is estimated that LBP has an incidence rate of 84% and a prevalence of 80% [Soto-Padilla et al., 2015] considered as the second cause of orthopedics visits.

Low back pain is considered an important affection in Ecuador as well, Fuseau et al. observed an increasing frequency of clinical consults related to LBP between 2017 and 2020 in a health care center N1 of Imbabura, Ecuador of 2055 patients specially in patients of working age groups with a cumulative frequency of 67.98% in ages between 28-60, it was determined that female groups had a higher overall incidence frequency than male groups, by comparison with international studies decrease of incidence frequency in groups above 60 years old was not clearly established [Fuseau et al., 2022].

2.1.1 Anatomical structure of the lumbar spine: a clinical approach.

The vertebral column is responsible for supporting weight, providing structural stability, as well as, protection and distribution of the spinal nerves. The human spine is formed by vertebrae and intervertebral discs and can be divided in the cervical, thoracic and lumbar regions in addition to the sacrum and coccyx bones[Mahadevan, 2018]. The vertebrae are the bony structures that form the backbone, each vertebra has a cylinder-shaped body, a vertebral arch (where the nerves of the spinal column are located) and a number of

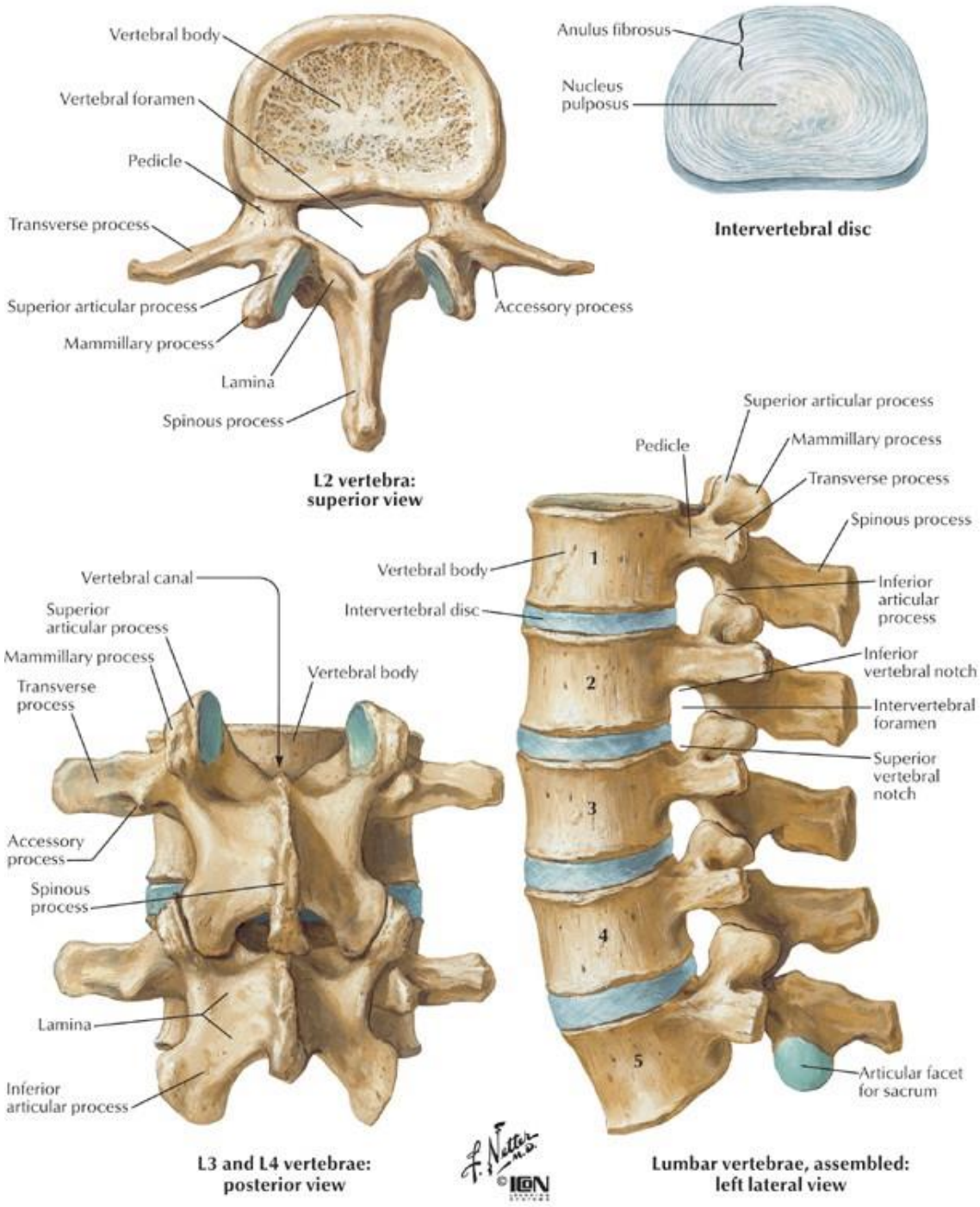

Figure 2.1: Anatomical structures of the lumbar spine, vertebral components and facet joint articulation, from [Chan, 2015]

processes that act as points of attachment for ligaments and muscles [Panjabi et al., 1992].

The cervical region of the spine is composed seven vertebrae denominated C1 to c7 to support the skull and jaw, in the thoracic region there are twelve vertebrae (T1-T12) that fuse with the ribs to give stability and protection to the internal organs and the lumbar region has five vertebrae (L1-L5) [Frost et al., 2019]. It has been shown that vertebrae become wider in thickness and depth towards the lumbar region to support the load of the cervical and thoracic segments [Inoue et al., 2020]. Intervertebral discs compose up to 30% of the vertebral column and as the name implies they can be found between each vertebrae, these fibrous avascular structures are formed by a gelatinous center known as the *nucleus pulposus* and a dense outside ring of fibrous cartilage named the *annulus fibrosus* serving the function of shock absorbers and allow spine movement, in the lumbar area, these discs have the largest surface area of the spine since this region is subjected to greater stress due to flexion movements, axial rotation and lateral bending [Frost et al., 2019, Raj, 2008]. Additionally other a series of muscular groups are found in the surrounding areas of the spine that provide mobility and help maintain balance.

Another important component located in the posterior of the spine are zygapophysial or facet joints that are synovial articulations comprised of the interaction of superior and inferior bone processes of the vertebrae that play an important role in load transmission across the spine, this articulations have a cartilage and biomechanical alterations may result in physical discomfort [Dreyer and Dreyfuss, 1996].

Biomechanics of the lumbar spine

The analysis of movement of the human spine is a complicated due to the interaction between small structures with different physical capabilities, the principal movements done by the the lumbar column include, see Figure 2.2:

- Extension motion, describes a movement in the direction of the anteroposterior section of the body across the sagittal plane, several studies report a displacement of2 up to 6 angle degrees in the transversal axis with around 40% of the compressive forces concentrated into the facet joints.

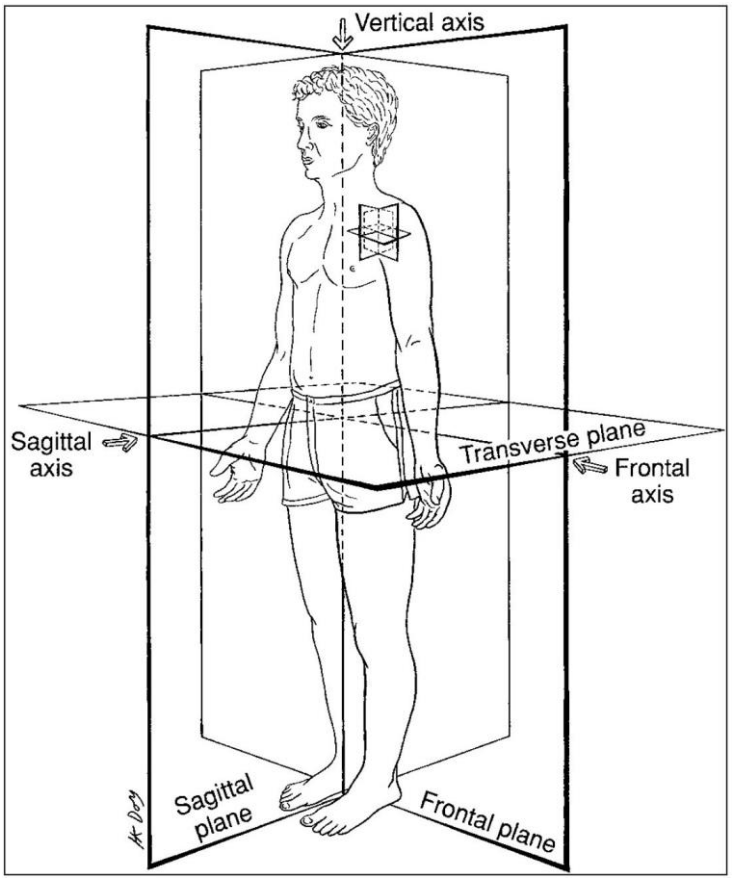

Figure 2.2: Anatomical division in planes and axes, from [Clarkson and Lippincott, 2021].

- Flexion motion, the upper body translates in a frontal displacement across the sagittal plane and articular components of vertebrae separates as far as 50 angle degrees from starting position, tension forces are focused posterior ligaments and muscles while compressive forces concentrate on intervertebral discs [Troup et al., 1968].

- Axial rotation, during this movement thoracic portion of the body rotates across the transversal plane up to 7.5 angle degrees, the movement is limited due to vertebral processes is limited to the available space for facet joint given the contacts between bone structures [Haughton et al., 2002].

- Lateral bending is a movement across the frontal plane in which the spine displaces across the vertical axis, little is known about this movement terms of effects of load across the lumbar structures [Frost et al., 2019].

2.1.2 Physiopathology of low back pain

The pathological source of LBP has been associated to multiple origins, across different investigations it has been stated that the majority of cases are related to muscle fiber disruption or ligament damage as a result of abrupt forces or weak muscles, generally is not a serious condition and common medication, and rest are enough to assure recovery [Urits et al., 2019, Peng, 2013].

Disc degeneration has proven to be a source of LBP, in fact, over the past decade numerous studies indicate that lumbar intervertebral disc degeneration is a multifactorial condition, that is caused by genetic and nutritional factors and mechanical factors [Cheung, 2010], degeneration of the intervertebral disc is considered as important source of pain in patients with low back pain. This disease influences the nervous system by stimulation of nociceptors in the anulus fibrosus and causing pain. When disc degeneration produces a disc herniation, the adjacent nervous system structures, can be altered, causing neuropathic pain. Disc deterioration also affect other spinal structures, such ligaments, muscles, and facet joints, which can also generate pain. In consequence, disc degeneration might be responsible for the chronic low back pain without being the actual pain focus [Brisby, 2006].

Disc herniation is a more serious condition and has known as one of the most common causes of low back pain. This pathology occurs for a protrusion of a lumbar intervertebral disc and some manifestations of pain and paresthesia in the area appears. These symptoms are due to rupture of the lumbar intervertebral disc for external forces as degeneration. Nevertheless, the cause and relationship of the lumbar disc herniation to back pain and sciatica have not been fully elucidated [Wang et al., 2021a]. Spondylosis is loss of the articular tissue and is characterized by narrowing or collapse of the disk space or arthritis of the facet joints [Elder and Witham, 2016].

Scoliosis is defined as a series of changes in the lumbar spine that maintain shoulder balance in the setting of pelvic obliquity. Numerous investigations revealed correlations between scoliosis, degenerative changes in the lumbar spine and low back pain. However, the relationship is not clear, resulting in limited evidence to guide treatment [Sheha et al., 2018].

Other important factor can be fractures of vertebral processes and vertebral bodies, that are product of a great force resulting in serious consequences given the presence of multiple nerve connections that go through the spine. It's highly important to identify patients undergoing serious pathology during a clinical examination like a vertebral fracture, that may require specific treatment. The clinical practices guideline suggests the use of red flags to screen serious causes of back pain as well as imaging techniques [Williams and Irwig, 2013].

One characteristic of LBP is that oftentimes can extend towards one or both of the lower limbs causing pain, this process is known as Radiculopathy and is a nerve inflammation of the nerves that combine in the sciatic nerve causing discomfort in the lower limbs [Frost and Brown, 2016].

Rare conditions linked to LBP symptomatology

Referred causes of LBP: Internal structures of the visceral organs constitute a risk factor producing referred pain that lead to distress in the lower back area. Aortic aneurysm is heavily linked to LBP and is considered a life threatening condition, acute pancreatitis and renal colic are indirect causes of LBP as well [Karnath, 2003].

Systemic causes of LBP: This are rare conditions such as inflammatory spondyloarthropathy, infections, and cancerous tumors. Since low back pain is one of the leading reasons for physician visits, in most cases distress comes from a benign etiology. But, in some cases physician examination is recommended to prevent aggravation of related pathologies [Karnath, 2003].

Diagnostic and prognosis methods

LBP is a frequent condition, acute cases in general present a favorable outcome for the patient, however, with the potential increase of risk factors some cases may transition from acute to chronic episodes that require more time and economical investment. It is important to promote the development of diagnostic tools and evaluation methods to provide better treatment [Patrick et al., 2014].

In order to diagnose patients, it is important to recompile information regarding the medical history of the patient: symptomatology (duration, timing, location, severity), comorbidity factors (metabolic disorders, hypertension, obesity, and so forth), previous

treatment [Tarabeih et al., 2022] and discard infections or any other disease via hematologic testing . Imaging techniques such as X-rays or magnetic resonance imaging MRI, tomography are not recommended due to the lack of specificity in terms of non specific discomfort, most patients recover in the first days even without treatment, still imaging methods are advised for structural fractures, herniated disk or infections. Physical examination is a highly important testing phase to determine possible causes: *spinal stenosis* (radiculopathy), *specific spinal instances* or *non-determined LBP* by means of evaluating the performance of the muscular structure of the lower segment of the body in specific trials for of neurological burden (Babinski sign, straight leg rise SLR, crossed SLR) [Patrick et al., 2014]. Range of motion (ROM) analysis is a common physician practice consisting of evaluating the angle of movement of joints, muscular weakness is associated with limited range of ROM values [Afonso et al., 2021]. The most common ROM test is the Schober Test and consist of calculating the difference in mobility changes using a taping measure, is considered an important element to designate therapy [Nattrass et al., 1999].

Diagnosis can be a frustrating process, especially for patients with nonspecific LBP given the multiple etiological factors involving the pathology and lack of sensitivity and specificity of state of the art methods: imaging methods have limitations and treatment exercises present better results during preventive phases [Grabois, 2005, Deyo and Weinstein, 2001], hence the importance of promoting new diagnostic and prognosis methods for precise detection of LBP with the combination of precise measurements technologies ROM assessment has gained attention in recent years along with the revolution of artificial intelligence in the medical field.

Conventional treatment

As described previously, low back pain is most often caused by muscle stiffness caused by weak muscles and other not so common causes such as fractures and viscerogenic failure. It is acknowledged that the majority of acute cases may disappear within 6 to 8 months with no required treatment. Some nonsurgical treatment options include physical therapy with stretching exercises to help decompress intervertebral discs and improve blood flow. Massage therapy, which can increase range of motion mobility, improve serotonin levels and reduce depression even on the long term [Hernandez-reif et al., 2001],

electrical stimulation of trans-cutaneous nerves, application of heat or cold temperatures, ultrasound therapy and chiropractics as well as the use of non-steroidal anti inflammatory drugs (NSAIDs) with oral or topical medications, although the application of medication reduces pain, there is no improvement in terms of functionally, it is recommended to avoid activities producing pain however immobilization is always recommended [Patrick et al., 2014, Malanga and Wolff, 2008].

If the condition is severely affecting the nerve edgings surgical options are recommended to relieve radiculopathies, some invasive options include: Discectomy is the gold standard procedure for corrective surgical procedure to correct LBP, in which a segment of the herniated disc is removed to reduce nerve stress. Laminectomy on the other hand is used to remove portions of spinal processes to leave more space for nerve structures. Microendoscopic discectomy is a new technique of minimal invasion using a needle-like tool to perform a discectomy [Berry et al., 2019].

2.2 Inertial sensor units

Motion capture (MoCap) is the process of acquiring information of living subjects in movement, standard methods are based on optical, magnetic and even sonic techniques with the purpose of quantifying kinematic and kinetic information of motion, the different types of technologies allows MoCap systems to be optimized in different areas [Aminian and Najafi, 2004] by means of camera based systems, inertial sensor units or hybrid systems [Menolotto et al., 2020]. The applications for detection and classification of physical pathological patterns with the analysis of specific movement features has gained relevance in recent years [Mannini et al., 2016] with the development of wearable inertial measuring units allowing data collection of long term activity in outside environments for postural recognition and pattern identification commonly used for gait analysis, orthopedics, sports and fall risk estimation [Aminian and Najafi, 2004]. Furthermore, MoCap technologies have wide applications in automotive, entertainment, construction, aerospace and healthcare industry [Menolotto et al., 2020].

Table 2.1: Properties and specifications of the NGIMUs from [Technologies, 2021]

Feature	Description	Specification
Accelerometer	Measures changes in velocity of a moving subject	Range: 16 g Sample range: 400Hz
Gyroscope	Measures changes in angular velocity	Range: 2000°/s Sample rate: 400Hz
Magnetometer	Measures relative changes in a magneitc field	Range: 1300 uT Sample rate: 20Hz

Inertial measurement units (IMUs) are small wearable sensors with three axial accelerometer, gyroscope and/or magnetometer that can be placed in multiple parts of the body [Ghislieri et al., 2019] using elastic straps to acquire information about movement performance. The model used in this investigation was the Next Generation inertial measurement units (NGIMU) by x-io Technologies (Figure 2.3) with compact sensing elements and free code algorithms, portable battery and memory sloth as well as wireless synchronization via Wi-Fi [Technologies, 2021].

Figure 2.3: Second generation of NGIMUs with charger and wireless connection stations by x-io Technologies, taken from [Technologies, 2021]

2.3 Artificial intelligence and medicine

New advances in the technology offer the capacity to improve the evaluation and prognostic of states of the movement and healthy of patients. These new technologies give the possibility of get data from long periods and learn about the changes in the time. The use of wearable devices with embedded sensors like inertial sensor can recollect data in any moment and store it in a database. Data raw can analyzed by algorithms where is it processed and classified [Jourdan et al., 2021]. Studies have been carried out using ROM

assessment with inertial sensors for industrial applications, Rabal-Pelay et. all evaluated forklift workers and office workers with spinal discomfort with statistical analysis to identify differences between groups and determinate alteration in the angles of movement for future personalized compensatory exercises [Rabal-Pelay et al., 2021].

New algorithms and system allow us explore new tools to physiotherapeutic in the monitoring evolution and rehabilitation of chronic diseases. It is because of continuous data recollection gives the possibility of excellent solution in the diagnosis of symptoms in any therapy path. New researches show the new approach in the data analysis with AI solutions. Examples of this approach is the research of [Pistolesi and Lazzerini, 2020] where used inertial sensor data to classify and improve lifting movement in workers to decrease the possibility of low back pain. The solution was to classify safety levels with a Neural Network, an interesting tool in the Machine Learning (ML). The machine learning solutions are the most used in the last decade because of it is able to relate sensor data and human body systems. Then, this information is interpreted by the machine and validated using statistic criteria. The importance of Machine Learning (ML) is the possibility of recognize patterns and classify them with the less human intervention by using a template model trained for a specific problem.

2.3.1 Machine learning

Machine learning (ML) is a branch of artificial intelligence that can be defined as the application of advanced statistical techniques to allow computers identify functional information to make more precise decisions. The analysis is based in automated identification of relationships between variables by managing to insert information (inputs) into an algorithm to process and obtain a desired answer in terms of outputs [Rajkomar et al., 2019]. In medicine many relationships have a clear relationship such as body mass index and diabetes [Sidey-Gibbons and Sidey-Gibbons, 2019], the applications of ML in medicine are vast in diagnosis, prognosis, treatment, and clinician work optimization. Clinical systems cannot provide a complete evaluation of patients given the amount of information, in terms of time but with the application of artificial intelligence in medical systems might provide a way to deeply analyze and extract information from the overwhelming amount of information [Rajkomar et al., 2019]. In general ML can be divided into two categories according

to the type of the information used for training:

Unsupervised learning the algorithm learns patterns using training data without being given explicit labels or outcomes in order to identify features in the data and to recognize patterns or correlations in the data, in essence the algorithm learns pattern data on its own.

Supervised learning is defined as the application of a model working with a data set trained with a known outcome associated to a defined features of interest, in other words the training data has categorical labels and the outcome is known. Supervised learning requires training data to predict outcomes based on the provided data, even with unprecedented inputs.

- ***Regression models*** Are commonly used to study the relationship between independent variables and one or more dependent variables, in simple terms the output is a continuous value and can even be used to predict future values.

- ***Classification models*** According to Saravan et al. machine learning supervised classifiers can be categorized into probabilistic classifiers (Naive Bayers Classifiers, Bayesian Network, Maximum entropy), linear models (Support Vector Machine, Liner regression, Decision tree, Neural network) [Saravanan and Sujatha, 2018] and other classifiers and in simple terms can be used to calculate the probability of a sample of being part of a category by establishing a relationship with independent variables [Sen et al., 2020].

For algorithm selection there are multiple algorithms with different capabilities for medicine. In a study made by Khubeb Siddiqui et al. it was concluded that the algorithms like decision forests have a high accuracy and are easier to understand the acquired results give the detailed logical thinking output whereas algorithms like support vector machines or artificial neural networks cannot generate logical rules although have high accuracy results, in this case we are looking for new ways of analyzing data coming from various sources like ECG, EEG and provide a viable tool for decision making, hence the importance of explaining the steps for the classification results [Siddiqui et al., 2020].

2.3.2 Classification models

This protect is focused only in supervised classification ML models, the seven algorithms selected were selected according to the methodology proposed by De la Torre, et. al:

Logistic regression: is used to calculate the probability of a categorize whether or not an event falls into category using independent variables to determine a a categorical dependent variable, considered one of the most popular methods Logistic regression can provide a binary output (0 or 1) [Boateng and Abaye, 2019].

Decision tree: this algorithm disposes the provided data in form of nodes, branches represent the decision rules based on the conditions of the data and leafs are the output [Song and Ying, 2015].

Random forest: is a classification and regression algorithm that uses multiple decision trees trained using subsets of data from the dataset, reducing overfitting and achieving better results by combining the results of all calculated trees [Biau and Scornet, 2016].

Support Vector Machines (SVM): is used to estimate a hyperplane (with dimensionality equal to the number of variables) that separates one variable category from the other with the biggest distance possible [Meyer and Wien, 2015].

K-nearest neighbors: is a simple non parametric algorithm that assumes similarity between the data to determine the categorical output [Taunk et al., 2019].

Multilayer perceptron: is a three layer supervised neural network composed of an input layer, a hidden layer and an output layer based in back propagation to predict the probability of an output of belonging to an specific category [Nosratabadi et al., 2021].

Gradient boosting algorithm (GBA): is a regression or classification model that combines weak models (such as decision trees) into an ensemble by calculating the gradient of loss function in each iteration repeatedly unlit obtaining a determined threshold value [Beygelzimer et al., 2015].

2.3.3 Verification tests

The outcomes of a classification model may be bicategorical, (one or zero, true or false) or multi categorical (excellent, good, bad) according to the requirements of the problem [Sen et al., 2020]. The present investigation is focused in evaluating the predictive ca-

pabilities of seven different ML models, according to bibliography it is recommended to use different testing scores according to the number of classifiers and number of data sets [Stapor, 2018].

Table 2.2: Confusion matrix of a prediction model

		Observed	
		Positive	*Negative*
Predicted	*Positive*	True Positive (TP)	False Positive (FP)
	Negative	False Negative (FN)	True Negative (TN)

In order to evaluate the quality of the results obtained from different classifiers there are several parameters that can be estimated using the confusion matrix using the correctly and incorrectly predicted values, as seen in the Table 2.2

- *Accuracy:* the term is used to estimate how close is the obtained value from the realvalue in a ML model and can be obtained using the following formula:

$$Accuracy = \frac{TP + TN}{TP + FN + TN + FP} \tag{2.1}$$

- *Precision:* is a statistical metric used to evaluate the true positives obtained dividedby the total of true positives and false positives:

$$Precision = \frac{TP}{TP + FP} \tag{2.2}$$

- *Sensitivity:* also known as Recall, is a metric used to estimate the ability of the model to obtain positive results among all the positive results and is calculated using [Metz, 1978]:

$$Sensitivity = \frac{TP}{TP + FN} \tag{2.3}$$

- *F-Measure or F-Score:* is calculated using the harmonical mean between the precision

and sensitivity with reciprocal values as shown below [Taha and Hanbury, 2015]:

$$F - Measure = \frac{2}{Precision + Sensitivity} = \frac{2TP}{2TP + FP + FN} \tag{2.4}$$

- *Matthews correlation coefficient (MCC):* also known as Phi coefficient establishes a correlation between the observed and predicted values The results can be -1 for a negative correlation, 0 for no correlation and 1 for a positive correlation

$$MCC = \frac{TP * TN - FP * FN}{\sqrt{(TP + FP)(TP + FN)(TN + FP)(TN + FN)}} \tag{2.5}$$

- *Area under the ROC curve:* The ROC curve is calculated using the True positive rate vs. The False positive rate, in binary model assessment is used as follows: the greater the area under the curve, the better the performance of the model.

- *Mean absolute error (MAE):* is the sum of all the absolute differences between the observed value and predicted value is divided by the total number of sample obser- vations [Willmott and Matsuura, 2005]:

$$MAE = \frac{1}{n}\sum_{i=1}^{n}|y_i - \bar{y}| \tag{2.6}$$

- *Root mean square error (RMSE):* is the square root of the mean absolute error. The advantage of using this method is the error has higher sensitivity to atypical values[Hyndman and Koehler, 2006]:

$$RMSE = \sqrt{\frac{1}{n}\sum_{i=1}^{n}|y_i - \bar{y}|} \tag{2.7}$$

2.4 Machine learning and motion capture: Related works

Several MoCap advances have been developed over the last decade, with three dimensional motion systems considered the gold standard, followed by inertial sensor units and lastly by optical sensor systems, each one has their pros and cons in terms of cost and accuracy results. In a study carried out by Washaunbaugh et al. concluded that inertial sensor units are both accurate and repeatable in gait spatiotemporal assessment concluding the similar results as other experiments in terms of Lin's concordance coefficient (LCC) and minimal detectable change (MDC) [Washabaugh et al., 2017].

Table 2.3: Resume of related work investigations of machine learning classification algorithms for disease applications

Comparative studies			
Algorithm type	**Disease**	**Accuracy**	**Reference**
Random Forest, SVM, and Naive Bayes	Lumbar radiculopathy	88.45%, 86.87% and 86.08%	[Sharif Bidabadi et al., 2019]
Linear regression and random forest	Knee osteoarthritis	72.2% and 74.1%	[Kwon et al., 2020]
Random Forest, Support Vector Machine, Decision Tree, and Logistic Regression	Parkinson's disease	78.69%, 74.75%, 66.89% and 63.93%	[Aram et al., 2017]
Logistic regression, Support vector machines, K-nearest neighbors, Gradient boosting, Decision trees, Random forest, and neural network algorithms	Cervical Pain Assessment	86.6%, 95.4%, 83.7%, 87.7%, 91.8%, 83.4% and 87.1%	[de la Torre et al., 2020]
K-nearest neighbors classifier and minimum distance classifier	NNAA	99.77%	[Switonski et al., 2019]
Support Vector Machine and Fruit fly optimization algorithm	Chronic kidney disease	98.50%	[Jerlin Rubini and Perumal, 2020]
Support Vector Machine	Gait for Neurological Disease	93.90%	[Wang et al., 2020]
Matlab based algorithm	Posture detection	94.90%	[Klishkovskaia et al., 2020]
Individual studies			
Algorithm type	**Disease**	**Accuracy**	**References**
Support Vector Machine	Wart Disease	97.70%	[TALABANI and Engin, 2018]
	Parkinson's Disease	91.10%	[Das et al., 2011]
Random Forest	Parkinson's Disease	94.60%	[Kuhner et al., 2017]

The application of motion sensors has gained interest due to possible industrial applications for postural behavior analysis in ergonomics risks related to shoulder and low back pain with relevant results for prevention of worker distress in warehouses [Zhao et al., 2022] The application of MoCap in low back pathologies has shown potential in the medical

field. Scholtes and colleagues reported a possible relation between lower limb mobility and LBP by comparing mobility angles and estimated distress on the lumbar area [Scholtes et al., 2009] and some other studies asses the validation and repeatability of motion capture technique for chronic and acute LBP assessment with marker-less motion capture systems showing promising results [Trinidad-Fernández et al., 2020]. However some factor to considerate when working with motion capture data is the high dimensionalityof multivariable information of three dimensional models that consistently is represented in non-linear models [Längkvist et al., 2014] which can be a challenge in automation with algorithm classification.

Respect with machine learning applications of spatiotemporal data acquired form MoCap technique for disease classification a few studies have presented the capabilities of algorithms in terms of algorithms, some other studies even compare the performance of algorithms for accurate classification of pathological conditions, see Table 2.3.

The present investigation was designed according to the work developed by the IDERGO investigation group from the University of Zaragoza who have developed a portable operative system compatible with inertial unit sensors denominated MoveHuman-Sensors (MH) with the purpose of improving biomechanical assessment of musculoskeletal activities with applications in health, spots or the industry. They have developed a work protocol based on physical evaluations of range of motion using different biomechanical testing systems [Marin, 2017].

Chapter 3

Methodology

3.1 Description of the Problem

Over the last decades the amount of medical information has increased exponentially and statistically the incidence cases of low back pain has doubled while the prevalence remains persistent. The development of medical tools to aid decision making can provide better outcomes for patients and optimize resources in the health care system, Fiigure 3.1.

3.2 Target definition

The objective of this phase was to obtain information that may determine a clear difference between pathological and healthy patients. It was necessary to recompile bibliographical information to set inclusion parameters for the variables needed in the investigation including age ranges, sex, geological location, clinical history (chronic, acute or subacute pain).

The inclusion parameters where individuals aged from 18 to 65 years old divided in two groups: a pathological group medically diagnosed with low back pain and a control group with no physical sign of pain. Participants were required to have no previous physiotherapy treatments in the past six months nor pharmacological drugs for pain treatment.

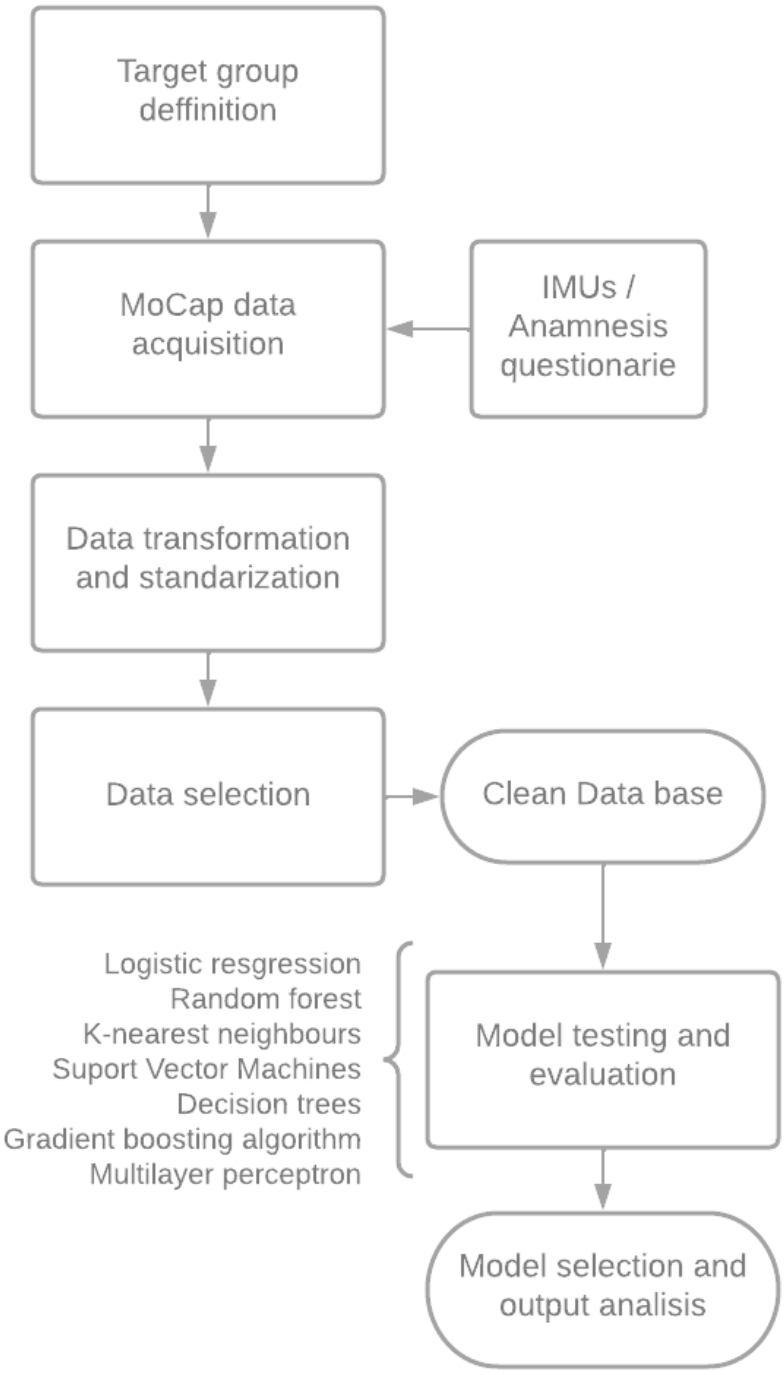

Figure 3.1: Methodology flowchart

3.3 Data acquisition

3.3.1 Ethics statement

Each patient was asked to sign a written informed consent containing information about the procedure and management. The protocol was developed according to the principles of the World Medical Association WMA Declaration of Helsinki and approved by the bioethics committee of the Pontifical Catholic University of Ecuador.

3.3.2 Data description

Information collected include variables such as: demographics (age, sex, height, body weight, body mass index) mainly acquired by filling an anamnesis form to register medical findings relevant to the investigation [Rodriguez, 1999]. Motion sensor information of spinal column articulation mobility in a three axial mobility assessment (flexion/extension, laterization and rotation). It is important to note all personal information from the patients was be kept in anonymity according to the ethics committee.

The experimental procedure for motion data acquisition consisted of positioning of three motion sensors: one in the forehead, one in the 7th cervical vertebra (C7) and one in the sacrum region using elastic harnesses, it is very important to properly adjust the harnesses tightly to the body of the patient, otherwise the sensor could register abnormal unwanted movements (Figure 3.2). For the purpose of evaluating functionality of the spinal column in three active range of movement exercises: flexion-extension, laterization and rotation. The patients were asked to perform 2 series of 7 repetitions for each exercise. In case of mistakes an additional series of repetition was performed by the subject.

The purpose of biomechanical assessment is to evaluate the functional capacity of the lower region of the spinal column in relation to the pelvis with the use of sensors. A set of repetitive movements are required to evaluate low back pain:

- Flexo-Extension: starting from a standing up position, the patient must lean forward with arms extended reaching for the toes, then moving back to a neutral standing position and finally leaning back all the way in the sagittal plane, as seen in Figure3.3.

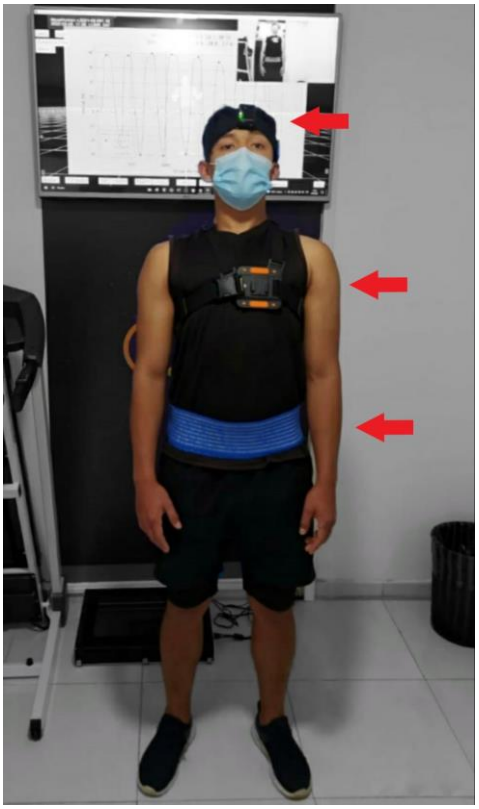

Figure 3.2: Harness positions for biomechanical assessment of male patient with motion sensors.

- Rotation: with arms close to the chest cavity the patient must perform lateral rotations going from left to right in the horizontal plane while keeping the waist fixed,shown in Figure 3.4.

- Laterization: in a standing position and with a straighten back the patient must perform lateral movements on the frontal plane, Figure 3.5.

The biomechanical assessment must be performed in a repetitive sequence of 6 cycles for each exercise, it is important to maintain uniform speed and constant performance reaching the maximum range of motion without discomfort. Exercises are performed with help of trained personnel to provide guidance in correct execution and operating the inertial sensor units.

Once the evaluation is finished the software provides a report with 45 variables (15 for each exercise) regarding angles, speed and acceleration in tables with reference values for consistency evaluation. Additionally graphs with maximum and minimum values, changes in angular velocity to help clinicians take decisions on better treatment [Marin, 2017].

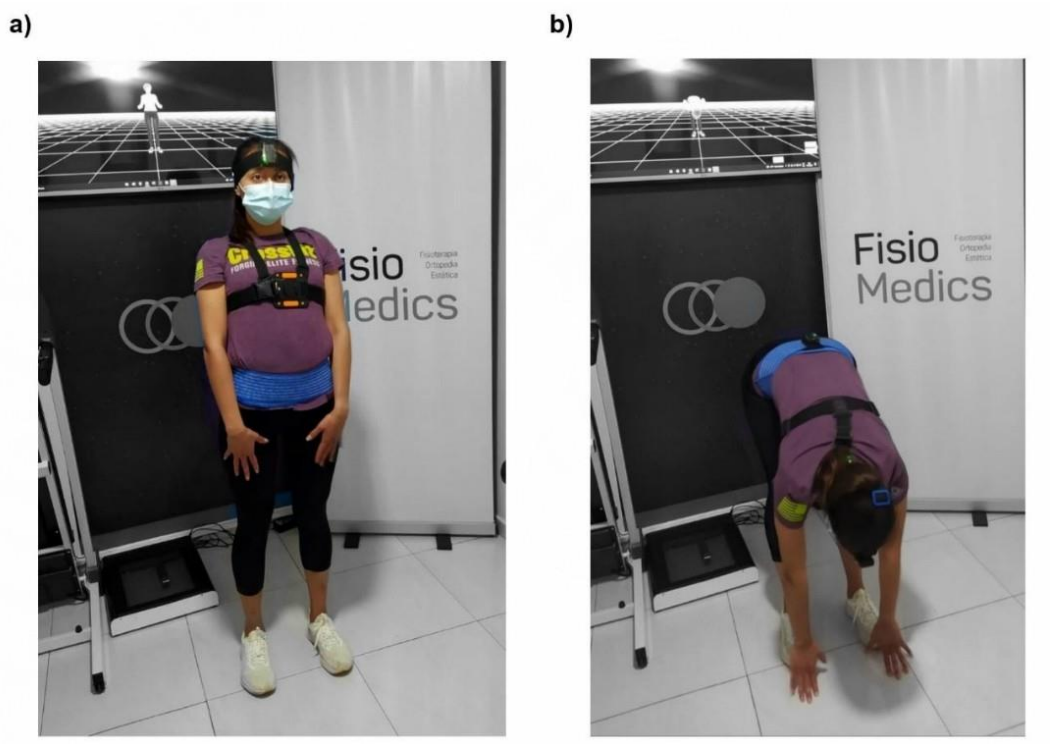

Figure 3.3: Flexo-Extension movement description: a) Extension position. b) Flexion position.

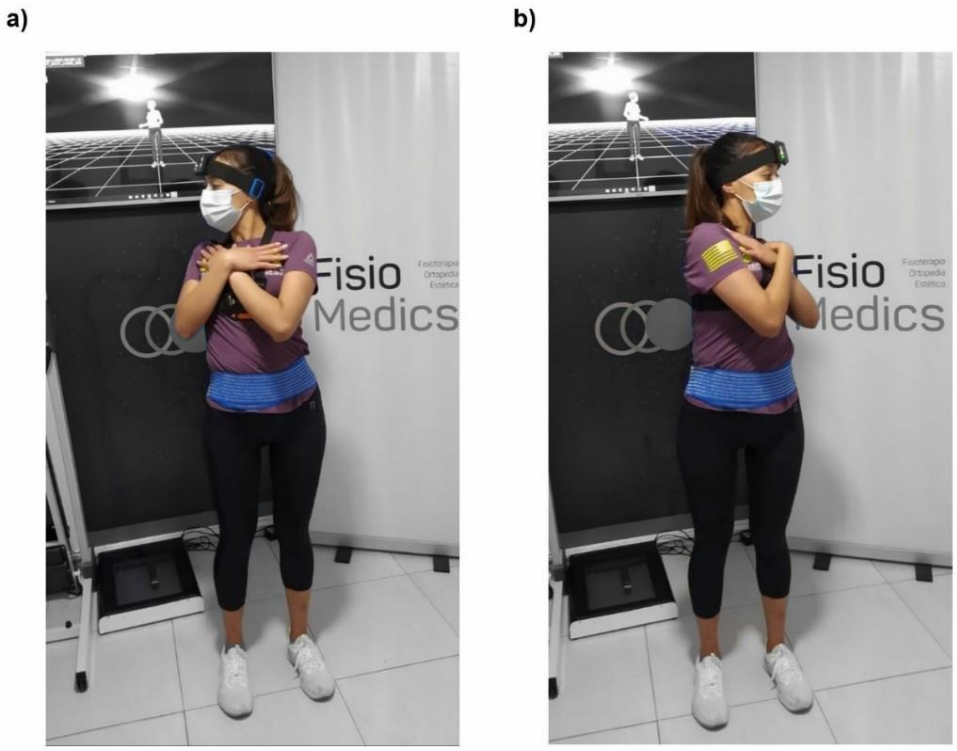

Figure 3.4: Description of the rotation movement a) Rotation towards the right side. b) Rotation towards the left side.

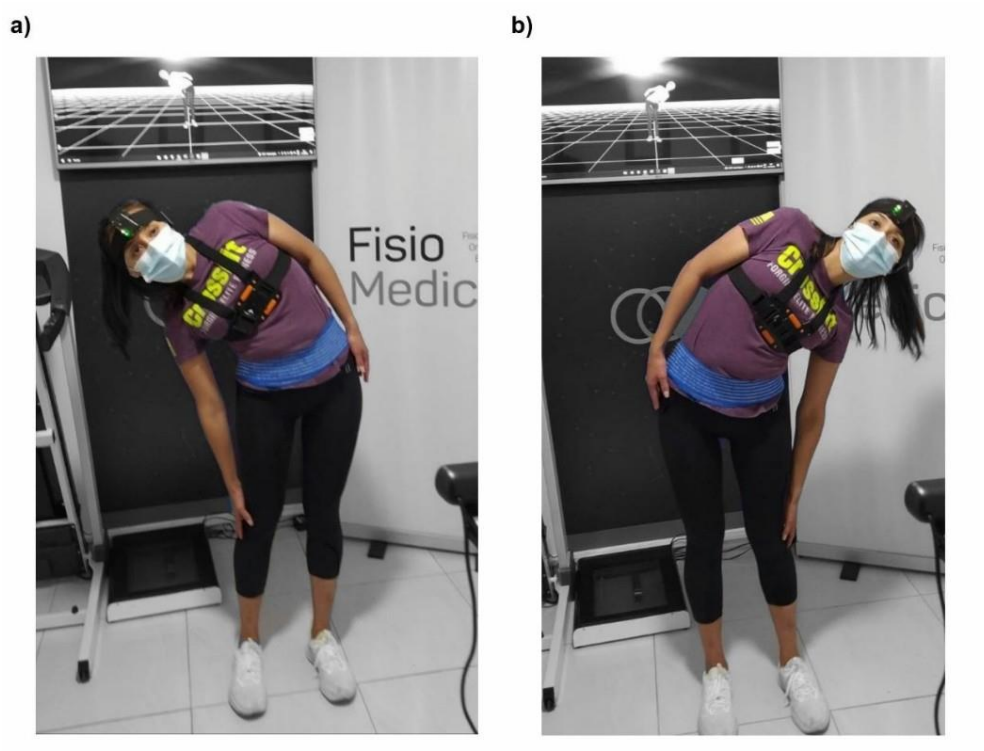

Figure 3.5: Laterization exercise description: a) Right body extension. b) Left body extension.

3.4 Data transformation and standardization

To reduce error in machine learning methods is important to homogenize the information available, such as working only with quantitative or qualitative data but not both or avoid complex variables composed of mathematical operations among simpler variables. In this study, after data set extraction each sample is organized for variable identification. It is necessary to convert of qualitative data from the anamnesis matrix into quantitative information. Furthermore, in this step it is essential to check the curve diagrams of patient movement generated by software MoveHuman to have a minimum of 6000 frame points and more than 6 peaks for angle as seen in Figure3.6, otherwise the program will not be able to calculate the movement of the patient (Annex .3).

3.5 Data selection

In this phase, it is important to perform a series of examination and correction techniques to eliminate non-consistent samples and reduce variables to avoid overparametrization of

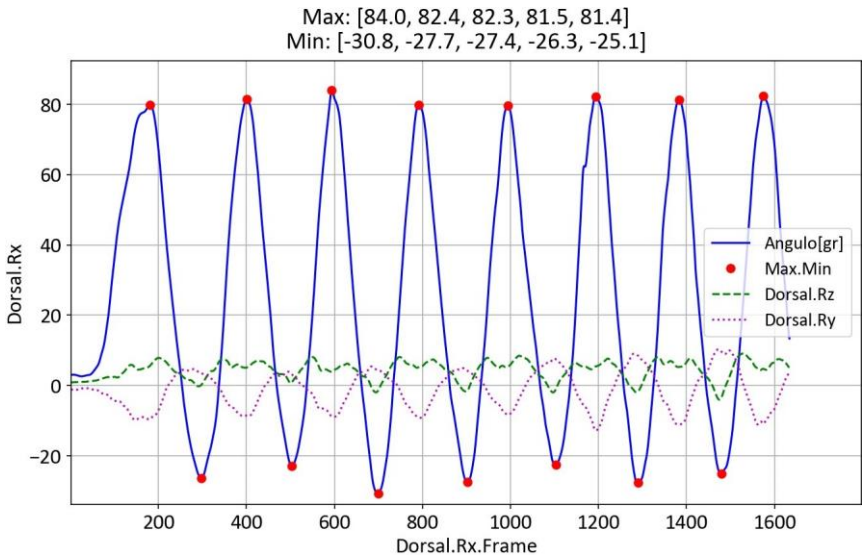

Figure 3.6: Curve diagrams of Flexo-Extension movement of a male patient. Positive values represent flexion phase and extension is represented by negative values.

the algorithms.

Sample selection: To evaluate the quality of acquired motion sensor samples, the acquired motion sensor data for the healthy and pathological groups is analyzed in the MoveHuman software. Abnormal values are expected as a result of sensor interference by inadequate exercise performance of the subjects, connectivity issues or presence of metallic objects. Filtration of non-usable samples such as incomplete series or missing values is necessary, for missing data the values are estimated using the group mean and samples with large portions of missing values can be eliminated to avoid bias.

Variable selection: The variables provided by the MH software are a total of 38 measures for each one of the exercises (Flexo/Extension, Rotation and Laterization):

- ***Angles:*** Length of the movement, angular velocity, maximum and minimum range,mean values, standard deviation and variation coefficient.
- ***Velocity:*** Maximum and minimum velocity, mean, standard deviation and variationcoefficient.
- ***Acceleration:*** Maximum and minimum acceleration, mean, standard deviation andvariation coefficient.

MoCaP data and clinical variables are integrated into a matrix for testing with ML

models. A total of 25 variables are divided as follows: 21 in MoCap variables (seven metrics for each exercise: Flexo/Extension, Rotation and Laterization) and 4 in clinical variables (age, sex, body mass index and educational level). An additional categorical variable was incorporated to predict the health status of a patient. It is important to remark that the number of variables was reduced with the purpose of avoiding overparameterization of the ML models by means of simplifying the information for the model, see Annex .4.

3.6 Model implementation and testing

The study focuses on the development of a medical tool to help medical professionals in the decision-making process. The tool uses classification algorithms to estimate a categorical variable, which indicates whether a patient is healthy or pathological. The algorithms that were used in this study are bases on 25 variables, which can be used to predict the health status of a patient.

This phase is focused in evaluating and comparing the performance of machine learning model categorization after training. The software WEKA, is an open-source program developed by the Waikato University based in Java does not require coding for machine learning applications. Also, it is important to mention that the final version of the data set needs to be converted into ".arff" file format for compatibility with machine learning analysis tools. Finally, when the data was loaded, it is ready for training and test analysis.

Classification models: seven different machine learning techniques are used for categorization of values for pathological or not-pathological with the objective of performance evaluation and parameter adjustment for optimum results as seen in Table 3.1.

3.7 Model evaluation and selection

A cross-validation technique was employed to evaluate the performance of the classification models used in the study. Each of the models was trained and tested using 10-fold cross-validation

The evaluation metrics obtained are precision, sensitivity, percentage of accuracy, F-measure, area under the ROC curve (AURC) and Matthew's correlation coefficient (MCC).

Table 3.1: Hyperparameter adjustment for each classification model

Classificator model	**Parameter adjustment**
Logistic Regression	Ridge Value in five segments from 1.0E-2 to 1.0E-10.
Desision tree	Confidence factor (0.15, 0.25, 0.35) and Instances per leaf (1,2,5,10,15,20).
Random Forest	Tree depth (0,1,2,3) and Number of trees (25, 50, 100, 150).
SVM	Complexity parameter (0.25, 0.5, 1, 1.5, 2). Tolerance 10.E-3. Kernel variation (Polykernel, Normalized Polykernel, RBF, PUK).
K-nearest neighbors	Distance metric: Euclidean, Manhattan and Filtered distance. Number of trees (5, 15, 15, 20, 30).
Multilayer perceptron	Momentum (0.1, 0.3, 0.5). Learning factor: in six segments from 0.1 to 0.8.
Gradient boosting	lLearning rate: 0.01, 0.1, 0.5, 1, 2, 3. Loss function: hinge loss and Log loss.

The error for each model was calculated using root mean squared error (RMSE) and mean absolute error (MAE).

Chapter 4

Results

4.1 Database results

For 6 months, 78 patients were evaluated through multiple series of repetitions of axial exercises using MoCap technology, of which 40 patients had been diagnosed with acute or chronic conditions and the remaining 38 patients presented no signs of LBP. A series of classification algorithms were trained and tested with 10-fold cross validation with the objective of automating categorical identification of pathological and healthy status. In this study, a total of 150 samples were selected with the intention of training machine learning (ML) models (Figure 4.1). To ensure the accuracy and reliability of the training results, the selected samples were separated in two groups: 75 samples for pathological patients and 75 samples for healthy patients. For every sample, 25 independent variables were used to the purpose of classify the dependent variable, of which the status of the patient was binary (pathological or healthy), for complete database see Annex .1.

4.2 Machine learning results

4.2.1 Classification models parameter adjustment

After performing the optimization of the parameters, the highest accuracy value corresponded to Support Vector Machine (SVM) with the 95.3% accuracy using a configuration of 1.5 in the complexity parameter and Pearson VII Universal Kernel (PUK). The following best model was the Multilayer perceptron with an accuracy of 92.67% using a configura-

Table 4.1: Resume of the 25 motion sensor and demographic variables after filtration of the database.

Type	Variable	Movement type
MoCap Data	Total Length (°)	Flexo-Extension Rotation Laterization
	Angular Velocity	
	Max Range	
	Max/Min Value	
	Max/Min Speed	
Demographics	Age, Sex, BMI, Educational level	

tion of Momentum: 0.5 and Learning factor of 0.8. Continued by the Random Forest classification with 92% accuracy with 150 trees and tree depth equal to zero. Next by the Logistic regression algorithm with 86.7% accuracy by adjusting the ridge value to 1.0^{-4} and batch size of 150. Then, the Gradient boosting algorithm achieved an accuracy rate of 82% by using a learning rate of 0.5 and hinge loss to determine the optimal hyperplane. Finally, both K-nearest neighbors and Decision tree obtained 81.3% accuracy using one instance per leaf with a confidence factor of 0.35 and a number of trees of 10 with filtered distances, respectively. These results are shown in Figure 5.1a-g. The results demonstrate the effectiveness of these algorithms in accurately classifying the dataset.

4.2.2 Machine learning model evaluation

Seven different classification algorithms were used to determinate their efficiency in accurately classifying the target variable as seen in the Table 4.3. The results showed that all models had and accuracy rate of over 80%. Nevertheless, after performing parameter optimization Support Vector Machine (SVM), Random Forest and Multilayer Perceptron (MLP) algorithms stood out as the most effective with accuracy rates exceeding 90%. A similar behavior is observed in sensitivity, precision and F-measure. Moreover, Random Forest, Logistic regression, SVM and Multilayer Perceptron had an Area Under the ROC curve (AURC) above 0.9 showing high reliability of the models based on the interactions of the obtained values from the Confusion matrix 2.2. With respect to error evaluation it found that the K-nearest neighbors algorithm had the highest mean squared error (MSE)

Table 4.2: Confusion matrix of the seven classification algorithms

Classifier Type	Actual value	Predicted value	
		Normal	Pathologicalal
Logistic Regression	Normal	66	9
	Pathological	11	64
Decision tree	Normal	60	15
	Pathological	13	62
Random Forest	Normal	70	5
	Pathological	7	68
SVM	Normal	75	0
	Pathological	7	68
K-nearest neighbors	Normal	61	14
	Pathological	14	61
Multilayer perceptron	Normal	71	4
	Pathological	7	68
Gradient boosting	Normal	61	14
	Pathological	13	62

Table 4.3: Classification machine learning algorithms metric results

Classifier Type	Accuracy (%)	Precision	Sensitivity	F-measure	AURC
Logistic Regression	86.67%	0.867	0.867	0.867	0.908
Decision tree	81.33%	0.814	0.813	0.813	0.859
Random Forest	92.00%	0.92	0.92	0.92	0.977
SVM	95.33%	0.957	0.953	0.953	0.953
K-nearest neighbors	81.33%	0.813	0.813	0.813	0.869
Multilayer perceptron	93.00%	0.927	0.927	0.927	0.936
Gradient boosting	82.00%	0.82	0.82	0.82	0.82

Table 4.4: Error evaluation of machine learning results

Classifier Type	Correct Class	Incorrect Class	MAE	RMSE	MCC
Logistic Regression	130	20	0.1523	0.3283	0.734
Desision tree	122	28	0.1937	0.4157	0.627
Random Forest	138	12	0.2269	0.2844	0.84
SVM	143	7	0.0467	0.216	0.911
K-nearest neighbors	122	28	0.3107	0.3958	0.627
Multilayer perceptron	139	11	0.1277	0.2755	0.854
Gradient boosting	123	27	0.1805	0.4243	0.64

value of 0.3, indicating an inferior predictive capability in comparison with the group. In addition, the Decision tree and Gradient boosting algorithms exhibited poor performance in terms of the root mean squared error (RMSE) and Matthews correlation coefficient (MCC), with the lowest recorded values as seen in the Table 4.4.

Chapter 5

Discussion

The algorithms that showed the best performance, with accuracy rates of over 90%, were the Random Forest, Support Vector Machine (SVM), and Multilayer Perceptron (MLP) after parameter optimization. These findings suggest that parameter optimization plays a crucial role in enhancing the performance of the classification algorithms. The high accuracy rates achieved by these models indicate their potential for use in various applications, such as disease diagnosis and classification, anomaly detection, and predictive modeling. Support Vector Machines (SVM) was consistently the best performing algorithm among the seven models tested with the highest statistical results in all metrics and lowest error for MAE and RMSE. Followed by Multilayer perceptron and Random forest which had very similar metric values, however although Multilayer perceptron presented a better accuracy, Random forest obtained a significantly better AURC which means that it can be considered a more reliable model than Multilayer perceptron. The remaining algorithms in general show a good performance with ¿80% accuracy.

The acquired results show a satisfactory performance for classification algorithms in the context of accuracy, precision, sensitivity, MAE and RMSE demonstrating viability of the analysis of spatiotemporal information originated from motion capture using machine learning tools. Regarding the application of classificators for abnormal range of ROM assessment of LBP, it's important to have the best possible performance to avoid the presence of false positive or false negatives given the importance of miss-classification in diagnosis and prognosis in the medical field. SVM was effortlessly the most feasible algorithm on account of its outstanding performance in comparison with the rest of the

algorithms.

One possible explanation for the obtained values of the classification models could be attributed to the limited sample size. With a small sample size, the variability of the data may not be fully captured, leading to the possibility of biased results. Although it would have been desirable to work with a larger sample size, due to the COVID-19 pandemic and the implementation of strict biosecurity measures in healthcare centers it was not possible to collect a larger sample, to solve this issue multiple exercise repetition per patient allowed to duplicate the data samples from the same subject and increasing algorithm training data. Despite this limitation, the obtained results are still significant and provide relevant information about the effectiveness of the different algorithms in classifying the dataset.

Another important factor to consider in building machine learning model is over-paramtetrization or underparametrization can seriously can affect the results, to solve this problem two measures are taken into account: variable reduction and hyperparameter adjustment for each one of the classification models. Working with inertial sensor units has an important beneficial factor, given the amount of sensors in multiple locations of the body in combination with multi-axial exercises during biomechanical assessment resulting in a significant amount of numerical information, however it can lead to overparametrization due to the high complexity of the data, hence the importance of correlation testing to evaluate the predictive capabilities of the independent variables respect the desired variable to discard unnecessary data, Weka offers integrated tools for variable predictive correlation ranking that simplify feature extraction, see Annex .2. But in addition to database optimization, hyperparameter optimization is the most important factor to determine the obtained results, several values for each model were tested, as seen in Figure 5.1 to obtain the best performing results. The present investigation propose a solution to increased parameter complexity in multidimensional time sequences produced by motion capture by using ML supervised classifiers to accurately identify abnormalities in ROM angles and provide a binary output of simple understanding for LBP assessment.

Nowadays ROM assessment is commonly performed with the Schober Test that uses measuring tapes or a double inclinometer to calculate the difference in ranges of movement from starting position to different displacement positions and just a few years ago the gold standard for measuring angular changes in the lumbar spine was using radiography images

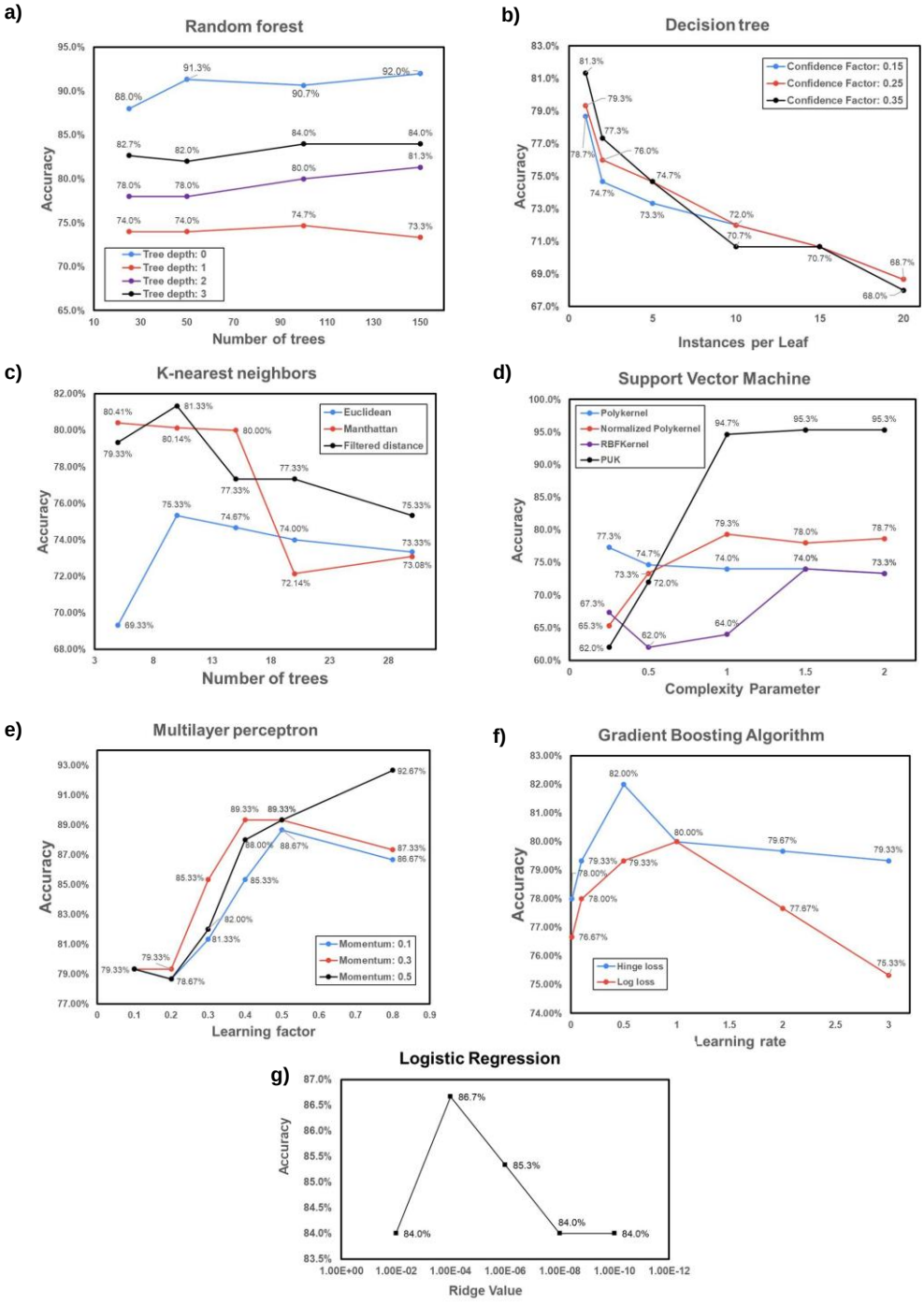

Figure 5.1: Performance plot of changes of hypperparameter optimization of the machine learning algorithms: a) Random Forest, b) Decision tree, c) K-nearest neighbors, d)Support Vector Machine, e)Multilayer Perceptron, f) GBA, g) Logistic regression.

to trace line for angle determination [Tousignant et al., 2005]. In this project inertial sensor units are incorporated to acquire precise spatiotemporal information with a noninvasive technique, thus allowing to incorporate machine learning applications. Given this is a very contemporary field very little is known about the applications of classification ML algorithmsto diagnose LBP or in coordination with MoCap data.

The present investigation was based in the work of De la Torre et. al that used a similar methodology for cervical spine assessment in the evaluation and comparison of ML techniques and the obtained results share similarities with the present study, proving the methodology can be viable and reproducible for biomechanical assessment of medical conditions related to the spinal column [de la Torre et al., 2020]. In addition to the methodology of Talabani et. al that evaluates the performance of SVM kernel type variations. Given that the achieved results of the present investigation share concordance with the previously described works we can presume the application of ML classificators in medicine are reproducible, however, it's important to remark that variation in results can be expected in classification techniques simply by employing a different dataset, hyperparameter testing is advised regardless of a close follow up methodology procedure. Some related studies have applied ML classificators demonstrating changes of parameters resulted in accuracy results variation, similarly for calculated error across different treatments for the same disease, parameter should be adjusted regardless [TALABANI and Engin, 2018].

The application of motion sensors for range of motion (ROM) evaluation offers the possibility to enhance the comprehension of LBP that still remains a highly difficult to identify the source in most of the cases treatment is administered with nonspecific diagnosis. The potential of MoCap in ROM analysis should be considered on the long term is an important field for better diagnosis and prevention of musculoskeletal diseases. For instance, several musculoskeletal factors involve the incidence of LBP, it has been stated that lateral flexion and hamstring restriction ROM are related to the increased chance of LBP [Sadler et al., 2017].

Some of the limitations of this work were that it wasn't possible to test the effectiveness of the classification results in real time with patients to evaluate the extends of clinical applicability in view of the fact that the classification models were tested and compared after MoCap data acquisition was complete due to data transformation and filtering. Addition-

ally the software tools MoveHuman and Weka heavily simplified data extraction and feature analysis but may be a limiting factor for reproducibility. Weka is a machine learning tool with several applications for classification, regression, clustering and more. Some studies have proven its utility for medical applications [Bharati et al., 2018, Findlow et al., 2008] and outperformed regular methods using machine learning for prediction of outcomes [Singal et al., 2013]. However an important disadvantage of using a non programming machine learning software is the reduction of parameter adjustment which is limited to the available options listed on the program.

Recommendations for future studies involve increasing the number of participants to assure a significantly large dataset and acquire better classification results in terms of the described metrics and errors, another consideration is to incorporate a pain/functionality questionnaire to explore additional variables of importance such as Roland-Morris questionarie or the Oswestry Low Back Pain Disability Questionnaire [Beattie and Maher, 1997], since MoCap data provides a vast amount of features with a nonlinear relationship, not all of them have a significant correlation and difficult a classification model construction, the addition of significant features relevant to LBP pathology may help improve obtained results.

Chapter 6

Conclusions

The origin of LBP is uncommonly understood before treatment assignment, new diagnostic tools are required to provide a better insight of the condition of patients and prevent transition from acute to chronic cases. Range of motion assessment or ROM can help to estimate the physical state of the articulations of the body, the most common practice is the Schober Test that uses a double inclinometers or measuring tapes to estimate angle changes in the lumbar spine. With the application of inertial sensor units it is possible to acquire reliable metrics of the biomechanical capabilities of the spine by performing multiaxial range movements, allowing to incorporate sophistical artificial intelligence techniques such as machine learning classificators with motion sensors demonstrating and effective automated alternative for identification of healthy vs. pathological patients with all ML models having >80% of accuracy. The most effective algorithms were SVM, Random forest and Multilayer perceptron that achieved more than 90% of accuracy.

MoveHuman and Weka software can heavily simplify the application of machine learning for several applications given its non-coding interface can provide fast analysis for classification and regression models, as well as feature extraction, is a great alternative for medical applications.

The application of machine learning tools in coordination with motion capture for biomechanical ROM assessment can successfully estimate the physical state of the articulations of the lumbar spine region, by combining the automation of data analysis using ML techniques, it is possible to obtain more efficient results that help in the diagnosis of patients with LBP. One of the potential applications of the present study is to establish a

metric for health insurance or physical rehabilitation centers and to establish a projection of economic investment per patient by optimization of the process by working in coordination with health care centers and increase the amount of available information.

6.0.1 Future works

Additional studies should focus on improve data collection and increase data samples for more ML precise model construction and inclusion of sophisticated techniques such as deep learning, new ML algorithms are appearing which presents better performances in the classification of patterns with automatically features extraction without human intervention. This type of ML algorithms is known as deep learning [Awais et al., 2021]. Some deep learning algorithms used are convolutional neural networks (CNN), recurrent neural networks (RNN) and long short-term memory (LSTM) networks and the incorporation of this tools may be included to help establish optimal patient rehabilitation with a personalized scope [Wang et al., 2021b]. Future work, is focused in the viability of the application of machine learning categorization of healthy and pathological state of muscle groups associated with movement in patients with LBP by means of using MoCap in multiaxial exercise characterization to enhance personalized physical therapy.

Bibliography

[Afonso et al., 2021] Afonso, J., Ramirez-Campillo, R., Moscão, J., Rocha, T., Zacca, R., Martins, A., Milheiro, A. A., Ferreira, J., Sarmento, H., and Clemente, F. M. (2021). Strength training versus stretching for improving range of motion: A systematic review and meta-analysis. *Healthcare*, 9(4):427.

[Aminian and Najafi, 2004] Aminian, K. and Najafi, B. (2004). Capturing human motion using body-fixed sensors: outdoor measurement and clinical applications. *Computer Animation and Virtual Worlds*, 15(2):79–94.

[Aram et al., 2017] Aram, K., Alhendi, M., Cao, Y., and Won, D. (2017). Speech signal classification for parkinson's disease diagnosis. In *IIE Annual Conference Proceedings, Pittsburg, Pennsylvania*, pages 1030–1035.

[Awais et al., 2021] Awais, M., Chiari, L., Ihlen, E. A., Helbostad, J. L., and Palmerini, L. (2021). Classical machine learning versus deep learning for the older adults free-living activity classification. *Sensors*, 21(14):4669.

[Ballina et al., 2000] Ballina, F., Carmona, L., Alonso, A., Álvaro-Gracia, J., Andreu, J., Rubiò, J., Collantes, E., and Cruz, J. (2000). Epidemiología de las enfermedades reumáticas. *Alonso A, Álvaro-Gracia JM, Andreu JL, Blanch i Rubiò J, Collantes E, Cruz J et al: Manual SER de las enfermedades reumáticas. Madrid: Médica Panamericana*.

[Beattie and Maher, 1997] Beattie, P. and Maher, C. (1997). The role of functional status questionnaires for low back pain. *Australian Journal of Physiotherapy*, 43(1):29–38.

[Berry et al., 2019] Berry, J. A., Elia, C., Saini, H. S., and Miulli, D. E. (2019). A review of lumbar radiculopathy, diagnosis, and treatment. *Cureus*, 11(10).

[Beygelzimer et al., 2015] Beygelzimer, A., Hazan, E., Kale, S., and Luo, H. (2015). Online gradient boosting. *Advances in neural information processing systems*, 28.

[Bharati et al., 2018] Bharati, S., Rahman, M. A., and Podder, P. (2018). Breast cancer prediction applying different classification algorithm with comparative analysis using weka. In *2018 4th International Conference on Electrical Engineering and Information Communication Technology (iCEEiCT)*, pages 581–584.

[Biau and Scornet, 2016] Biau, G. and Scornet, E. (2016). A random forest guided tour. *Test*, 25:197–227.

[Boateng and Abaye, 2019] Boateng, E. Y. and Abaye, D. A. (2019). A review of the logistic regression model with emphasis on medical research. *Journal of data analysis and information processing*, 7(4):190–207.

[Brisby, 2006] Brisby, H. (2006). Pathology and possible mechanisms of nervous system response to disc degeneration. *JBJS*, 88(suppl 2):68–71.

[Carpio et al., 2018] Carpio, R., Goicochea-Lugo, S., Chávez Corrales, J., Santayana Calizaya, N., Collins, J. A., Robles Recalde, J., Henández, A. V., Piscoya, A., Suárez Moreno, V., and Timaná-Ruiz, R. (2018). Guía de práctica clínica para el diagnóstico y tratamiento de lumbalgia aguda y subaguda en el seguro social del perú (essalud). In *Anales de la Facultad de Medicina*, volume 79, pages 351–359. UNMSM. Facultad de Medicina.

[Chan, 2015] Chan, H. Y. (2015). Lumbar vertebrae.

[Cheung, 2010] Cheung, K. M. (2010). The relationship between disc degeneration, low back pain, and human pain genetics. *The Spine Journal*, 10(11):958–960.

[Clarkson and Lippincott, 2021] Clarkson, H. M. and Lippincott, W. (2021). *"Musculoskeletal Assessment Joint Motion and muscle testing"*. Wolters Kluwer/Lippincott Williams amp; Wilkins Health.

[Das et al., 2011] Das, S., Trutoiu, L., Murai, A., Alcindor, D., Oh, M., De la Torre, F., and Hodgins, J. (2011). Quantitative measurement of motor symptoms in parkinson's

disease: A study with full-body motion capture data. In *2011 Annual International Conference of the IEEE Engineering in Medicine and Biology Society*, pages 6789–6792.

[de la Torre et al., 2020] de la Torre, J., Marin, J., Ilarri, S., and Marin, J. J. (2020). Applying machine learning for healthcare: A case study on cervical pain assessment with motion capture. *Applied Sciences*, 10(17).

[Deyo and Weinstein, 2001] Deyo, R. A. and Weinstein, J. N. (2001). Low back pain. *N. Engl. J. Med.*, 344(5):363–370.

[Dreyer and Dreyfuss, 1996] Dreyer, S. J. and Dreyfuss, P. H. (1996). Low back pain and the zygapophysial (facet) joints. *Archives of Physical Medicine and Rehabilitation*, 77(3):290–300.

[Elder and Witham, 2016] Elder, B. D. and Witham, T. F. (2016). Low back pain and spondylosis. In *Seminars in neurology*, volume 36, pages 456–461. Society of Indian Hand & Microsurgeons.

[Findlow et al., 2008] Findlow, A., Goulermas, J., Nester, C., Howard, D., and Kenney, L. (2008). Predicting lower limb joint kinematics using wearable motion sensors. *Gait Posture*, 28(1):120–126.

[Frost et al., 2019] Frost, B., Camarero-Espinosa, S., and Foster, E. (2019). Materials for the spine: Anatomy, problems, and solutions. *Materials*, 12(2):253.

[Frost and Brown, 2016] Frost, L. R. and Brown, S. H. (2016). Neuromuscular ultrasound imaging in low back pain patients with radiculopathy. *Manual Therapy*, 21:83–88.

[Fuseau et al., 2022] Fuseau, M., Garrido, D., and Toapanta, E. (2022). Caracter´ısticas de los pacientes con lumbalgia atendidos en un centro de atención primaria en ecuador.

[Ghislieri et al., 2019] Ghislieri, M., Gastaldi, L., Pastorelli, S., Tadano, S., and Agostini, V. (2019). Wearable inertial sensors to assess standing balance: A systematic review. *Sensors*, 19(19).

[Grabois, 2005] Grabois, M. (2005). Management of chronic low back pain. *American journal of physical medicine & rehabilitation*, 84(3):S29–S41.

[Hartvigsen et al., 2018] Hartvigsen, J., Hancock, M. J., Kongsted, A., Louw, Q., Ferreira, M. L., Genevay, S., Hoy, D., Karppinen, J., Pransky, G., Sieper, J., Smeets, R. J., Underwood, M., Buchbinder, R., Hartvigsen, J., Cherkin, D., Foster, N. E., Maher, C. G., Underwood, M., van Tulder, M., Anema, J. R., Chou, R., Cohen, S. P., Menezes Costa, L., Croft, P., Ferreira, M., Ferreira, P. H., Fritz, J. M., Genevay, S., Gross, D. P., Hancock, M. J., Hoy, D., Karppinen, J., Koes, B. W., Kongsted, A., Louw, Q., Öberg, B., Peul, W. C., Pransky, G., Schoene, M., Sieper, J., Smeets, R. J., Turner, J. A., and Woolf, A. (2018). What low back pain is and why we need to pay attention. *The Lancet*, 391(10137):2356–2367.

[Haughton et al., 2002] Haughton, V. M., Rogers, B., Meyerand, M. E., and Resnick, D. K. (2002). Measuring the axial rotation of lumbar vertebrae in vivo with mr imaging. *American journal of neuroradiology*, 23(7):1110–1116.

[Hernandez-reif et al., 2001] Hernandez-reif, M., Field, T., Krasnegor, J., and Theakston, H. (2001). Lower back pain is reduced and range of motion increased after massage therapy. *International Journal of Neuroscience*, 106(3-4):131–145. PMID: 11264915.

[Hoy et al., 2010] Hoy, D., Brooks, P., Blyth, F., and Buchbinder, R. (2010). The epidemiology of low back pain. *Best practice research. Clinical rheumatology*, 24:769–81.

[Hyndman and Koehler, 2006] Hyndman, R. J. and Koehler, A. B. (2006). Another look at measures of forecast accuracy. *International journal of forecasting*, 22(4):679–688.

[Inoue et al., 2020] Inoue, N., Or´ıas, A. A. E., and Segami, K. (2020). Biomechanics of the lumbar facet joint. *Spine Surgery and Related Research*, 4(1):1–7.

[Jerlin Rubini and Perumal, 2020] Jerlin Rubini, L. and Perumal, E. (2020). Efficient classification of chronic kidney disease by using multi-kernel support vector machine and fruit fly optimization algorithm. *International Journal of Imaging Systems and Technology*, 30(3):660–673.

[Jourdan et al., 2021] Jourdan, T., Debs, N., and Frindel, C. (2021). The contribution of machine learning in the validation of commercial wearable sensors for gait monitoring in patients: a systematic review. *Sensors*, 21(14):4808.

[Karnath, 2003] Karnath, B. (2003). Clinical signs of low back pain. *Hospital physician*, 39(5):39–44.

[Katz, 2004] Katz, S. I. (2004). Boning up for health: The national bone and joint decade. *Journal of Bone and Mineral Research*, 19(10):1605–1606.

[Klishkovskaia et al., 2020] Klishkovskaia, T., Aksenov, A., Sinitca, A., Zamansky, A., Markelov, O. A., and Kaplun, D. (2020). Development of classification algorithms for the detection of postures using non-marker-based motion capture systems. *Applied Sciences*, 10(11).

[Kuhner et al., 2017] Kuhner, A., Schubert, T., Cenciarini, M., Wiesmeier, I. K., Coenen, V. A., Burgard, W., Weiller, C., and Maurer, C. (2017). Correlations between motor symptoms across different motor tasks, quantified via random forest feature classification in parkinson's disease. *Frontiers in neurology*, 8:607.

[Kwon et al., 2020] Kwon, S. B., Ku, Y., Han, H.-S., Lee, M. C., Kim, H. C., and Ro, D. H. (2020). A machine learning-based diagnostic model associated with knee osteoarthritis severity. *Scientific Reports*, 10(1):15743.

[Leac et al., 2022] Leac, C. C., Méndez, D. M., Parreño, S. G., Navarro, B. G., Segura, G. M., and Grandes, R. M. (2022). Epidemiolog´ıa y riesgo de hernia discal lumbar en trabajadores activos. *Revista española de cirugía osteoarticular*, 57(290):3.

[Längkvist et al., 2014] Längkvist, M., Karlsson, L., and Loutfi, A. (2014). A review of unsupervised feature learning and deep learning for time-series modeling. *Pattern Recognition Letters*, 42:11–24.

[Mahadevan, 2018] Mahadevan, V. (2018). Anatomy of the vertebral column. *Surgery (Oxford)*, 36(7):327–332.

[Malanga and Wolff, 2008] Malanga, G. and Wolff, E. (2008). Evidence-informed management of chronic low back pain with nonsteroidal anti-inflammatory drugs, muscle relaxants, and simple analgesics. *The Spine Journal*, 8(1):173–184.

[Manchikanti, 2000] Manchikanti, L. (2000). Epidemiology of low back pain. *Pain physician*, 3(2):167–192.

[Mannini et al., 2016] Mannini, A., Trojaniello, D., Cereatti, A., and Sabatini, A. M. (2016). A machine learning framework for gait classification using inertial sensors: Application to elderly, post-stroke and huntington's disease patients. *Sensors*, 16(1).

[Marin, 2017] Marin, J. J. (2017). Sistema mh-fce (funcional capacity evaluation). evaluación de la capacidad funcional.

[Menolotto et al., 2020] Menolotto, M., Komaris, D.-S., Tedesco, S., O'Flynn, B., and Walsh, M. (2020). Motion capture technology in industrial applications: A systematic review. *Sensors*, 20(19).

[Metz, 1978] Metz, C. E. (1978). Basic principles of roc analysis. In *Seminars in nuclear medicine*, volume 8, pages 283–298. Elsevier.

[Meyer and Wien, 2015] Meyer, D. and Wien, F. (2015). Support vector machines. *The Interface to libsvm in package e1071*, 28:20.

[Nattrass et al., 1999] Nattrass, C. L., Nitschke, J. E., Disler, P. B., Chou, M. J., and Ooi, K. T. (1999). Lumbar spine range of motion as a measure of physical and functional impairment: an investigation of validity. *Clinical Rehabilitation*, 13(3):211–218.

[Nosratabadi et al., 2021] Nosratabadi, S., Ardabili, S., Lakner, Z., Mako, C., and Mosavi, A. (2021). Prediction of food production using machine learning algorithms of multilayer perceptron and anfis. *Agriculture*, 11(5).

[Ordoñez-Hinojos et al., 2012] Ordoñez-Hinojos, A., Durán-Hernández, S., Hernández-López, J., and Castillejos-López, M. (2012). Asociación entre actividad laboral con gran demanda de esfuerzo f´ısico y lumbalgia. *Acta Ort Mex*, 26(1):21–9.

[PAHO, 2019] PAHO (2019). Epidemiolog´ıa.

[Panjabi et al., 1992] Panjabi, M. M., Goel, V., Oxland, T., Takata, K., Duranceau, J., Krag, M., and Price, M. (1992). Human lumbar vertebrae. quantitative three-dimensional anatomy. *Spine*, 17(3):299–306.

[Patrick et al., 2014] Patrick, N., Emanski, E., and Knaub, M. A. (2014). Acute and chronic low back pain. *Medical Clinics of North America*, 98(4):777–789. Common Musculoskeletal Problems in the Ambulatory Setting.

[Peng, 2013] Peng, B.-G. (2013). Pathophysiology, diagnosis, and treatment of discogenic low back pain. *World journal of orthopedics*, 4(2):42.

[Pistolesi and Lazzerini, 2020] Pistolesi, F. and Lazzerini, B. (2020). Assessing the risk of low back pain and injury via inertial and barometric sensors. *IEEE Transactions on Industrial Informatics*, 16(11):7199–7208.

[Rabal-Pelay et al., 2021] Rabal-Pelay, J., Cimarras-Otal, C., Marcen-Cinca, N., Alcázar-Crevillén, A., Laguna-Miranda, C., and Bataller-Cervero, A. V. (2021). Assessment of spinal range of motion and musculoskeletal discomfort in forklift drivers. a cross-sectional study. *International Journal of Environmental Research and Public Health*, 18(6):2947.

[Raj, 2008] Raj, P. P. (2008). Intervertebral disc: anatomy-physiology-pathophysiology-treatment. *Pain Practice*, 8(1):18–44.

[Rajkomar et al., 2019] Rajkomar, A., Dean, J., and Kohane, I. (2019). Machine learning in medicine. *New England Journal of Medicine*, 380(14):1347–1358. PMID: 30943338.

[Rodriguez, 1999] Rodriguez, P. L. (1999). Principios técnicos para realizar la anamnesis - sld.cu.

[Sadler et al., 2017] Sadler, S. G., Spink, M. J., Ho, A., De Jonge, X. J., and Chuter, V. H. (2017). Restriction in lateral bending range of motion, lumbar lordosis, and hamstring flexibility predicts the development of low back pain: a systematic review of prospective cohort studies. *BMC musculoskeletal disorders*, 18:1–15.

[Saravanan and Sujatha, 2018] Saravanan, R. and Sujatha, P. (2018). A state of art techniques on machine learning algorithms: A perspective of supervised learning approaches in data classification. In *2018 Second International Conference on Intelligent Computing and Control Systems (ICICCS)*, pages 945–949.

[Scholtes et al., 2009] Scholtes, S. A., Gombatto, S. P., and Van Dillen, L. R. (2009). Differences in lumbopelvic motion between people with and people without low back pain during two lower limb movement tests. *Clinical Biomechanics*, 24(1):7–12.

[Sen et al., 2020] Sen, P. C., Hajra, M., and Ghosh, M. (2020). Supervised classification algorithms in machine learning: A survey and review. In Mandal, J. K. and Bhattacharya, D., editors, *Emerging Technology in Modelling and Graphics*, pages 99–111, Singapore. Springer Singapore.

[Sharif Bidabadi et al., 2019] Sharif Bidabadi, S., Murray, I., Lee, G. Y. F., Morris, S., and Tan, T. (2019). Classification of foot drop gait characteristic due to lumbar radiculopathy using machine learning algorithms. *Gait Posture*, 71:234–240.

[Sheha et al., 2018] Sheha, E. D., Steinhaus, M. E., Kim, H. J., Cunningham, M. E., Fragomen, A. T., and Rozbruch, S. R. (2018). Leg-length discrepancy, functional scoliosis, and low back pain. *JBJS reviews*, 6(8):e6.

[Siddiqui et al., 2020] Siddiqui, M. K., Morales-Menendez, R., Huang, X., and Hussain, N. (2020). A review of epileptic seizure detection using machine learning classifiers. *Brain informatics*, 7(1):1–18.

[Sidey-Gibbons and Sidey-Gibbons, 2019] Sidey-Gibbons, J. A. and Sidey-Gibbons, C. J. (2019). Machine learning in medicine: a practical introduction. *BMC medical research methodology*, 19:1–18.

[Singal et al., 2013] Singal, A. G., Mukherjee, A., Elmunzer, B. J., Higgins, P. D., Lok, A. S., Zhu, J., Marrero, J. A., and Waljee, A. K. (2013). Machine learning algorithms outperform conventional regression models in predicting development of hepatocellular carcinoma. *The American journal of gastroenterology*, 108(11):1723.

[Song and Ying, 2015] Song, Y.-Y. and Ying, L. (2015). Decision tree methods: applications for classification and prediction. *Shanghai archives of psychiatry*, 27(2):130.

[Soto-Padilla et al., 2015] Soto-Padilla, M., Espinosa-Mendoza, R., Sandoval-Garc´ıa, J., and Gómez-García, F. (2015). Frecuencia de lumbalgia y su tratamiento en un hospital privado de la ciudad de méxico. *Acta ortopédica mexicana*, 29(1):40–45.

[Stapor, 2018] Stapor, K. (2018). Evaluating and comparing classifiers: Review, some recommendations and limitations. In Kurzynski, M., Wozniak, M., and Burduk, R., editors, *Proceedings of the 10th International Conference on Computer Recognition Systems CORES 2017*, pages 12–21, Cham. Springer International Publishing.

[Switonski et al., 2019] Switonski, A., Josinski, H., and Wojciechowski, K. (2019). Dynamic time warping in classification and selection of motion capture data. *Multidimensional Systems and Signal Processing*, 30:1437–1468.

[Taha and Hanbury, 2015] Taha, A. A. and Hanbury, A. (2015). Metrics for evaluating 3d medical image segmentation: analysis, selection, and tool. *BMC medical imaging*, 15(1):1–28.

[TALABANI and Engin, 2018] TALABANI, H. and Engin, A. (2018). Impact of various kernels on support vector machine classification performance for treating wart disease. In *2018 International Conference on Artificial Intelligence and Data Processing (IDAP)*, pages 1–6. IEEE.

[Tarabeih et al., 2022] Tarabeih, N., Kalinkovich, A., Shalata, A., Cherny, S. S., and Livshits, G. (2022). Deciphering the causal relationships between low back pain complications, metabolic factors, and comorbidities. *Journal of Pain Research*, 15:215.

[Taunk et al., 2019] Taunk, K., De, S., Verma, S., and Swetapadma, A. (2019). A brief review of nearest neighbor algorithm for learning and classification. In *2019 International Conference on Intelligent Computing and Control Systems (ICCS)*, pages 1255–1260. IEEE.

[Technologies, 2021] Technologies, x.-i. (2021). Ngimu.

[Tousignant et al., 2005] Tousignant, M., Poulin, L., Marchand, S., Viau, A., and Place, C. (2005). The modified–modified schober test for range of motion assessment of lumbar flexion in patients with low back pain: A study of criterion validity, intra-and inter-rater reliability and minimum metrically detectable change. *Disability and rehabilitation*, 27(10):553–559.

[Trinidad-Fernández et al., 2020] Trinidad-Fernández, M., Beckwée, D., Cuesta-Vargas, A., González-Sánchez, M., Moreno, F.-A., González-Jiménez, J., Joos, E., and Vaes, P. (2020). Validation, reliability, and responsiveness outcomes of kinematic assessment with an rgb-d camera to analyze movement in subacute and chronic low back pain. *Sensors*, 20(3).

[Troup et al., 1968] Troup, J., Hood, C., and Chapman, A. (1968). Measurements of the sagittal mobility of the lumbar spine and hips. *Rheumatology*, 9(8):308–321.

[Urits et al., 2019] Urits, I., Burshtein, A., Sharma, M., Testa, L., Gold, P. A., Orhurhu, V., Viswanath, O., Jones, M. R., Sidransky, M. A., Spektor, B., et al. (2019). Low back pain, a comprehensive review: pathophysiology, diagnosis, and treatment. *Current pain and headache reports*, 23:1–10.

[Wang et al., 2020] Wang, L., Sun, Y., Li, Q., Liu, T., and Yi, J. (2020). Two shank-mounted imus-based gait analysis and classification for neurological disease patients. *IEEE Robotics and Automation Letters*, 5(2):1970–1976.

[Wang et al., 2021a] Wang, P., Chen, C., Zhang, Q.-H., Sun, G.-D., Wang, C.-A., and Li, W. (2021a). Retraction of lumbar disc herniation achieved by noninvasive techniques: A case report. *World Journal of Clinical Cases*, 9(27):8082.

[Wang et al., 2021b] Wang, Y., Zhang, N., and Chen, X. (2021b). A short-term residential load forecasting model based on lstm recurrent neural network considering weather features. *Energies*, 14(10):2737.

[Washabaugh et al., 2017] Washabaugh, E. P., Kalyanaraman, T., Adamczyk, P. G., Claflin, E. S., and Krishnan, C. (2017). Validity and repeatability of inertial measurement units for measuring gait parameters. *Gait Posture*, 55:87–93.

[Williams and Irwig, 2013] Williams, CM, H. N. M. C. v. T. M. K. B. M. P. and Irwig, L. (2013). Red flags to screen for vertebral fracture in patients presenting with low-back pain. *Cochrane Database of Systematic Reviews*, (1).

[Willmott and Matsuura, 2005] Willmott, C. J. and Matsuura, K. (2005). Advantages of the mean absolute error (mae) over the root mean square error (rmse) in assessing average model performance. *Climate research*, 30(1):79–82.

[Zhao et al., 2022] Zhao, Y. S., Jaafar, M. H., Mohamed, A. S. A., Azraai, N. Z., and Amil, N. (2022). Ergonomics risk assessment for manual material handling of warehouse activities involving high shelf and low shelf binning processes: Application of marker-based motion capture. *Sustainability*, 14(10).

Appendices

.1 Annex: Complete dataset of 150 samples

51	117.50065	65.7039982	94.2778518	66.4922971	-27.785555	188.864484	-135.16154	-0.7103247	75.6528239	52.1144596	63.3339758	27.8470721	-35.486904	120.848611	-106.756	-0.7078699	90.8815563	63.332095	74.0528613	33.5349733	-40.517888	106.412787	-104.08401	-0.8660094	100	45	23.1713088	3	0
52	115.55458	55.9135065	88.577673	73.2512481	-15.326425	121.698882	-114.54308	-0.7115241	115.617591	62.8356471	90.5002403	44.0565009	-46.443739	129.801575	-129.99481	-0.8031049	109.804898	49.5360444	77.3755657	41.0521844	-36.323381	105.077686	-91.473662	-0.7588988	100	23	21.9085299	2	0
53	156.432331	46.3961435	116.47459	94.5786472	-21.895943	124.803979	-122.31394	-0.6506069	106.439274	45.8789975	82.148437	40.5403003	-41.608137	86.2898944	-86.549687	-0.7450806	64.128489	29.9199793	53.2253009	28.331554	-24.893747	50.1976666	-53.955073	-0.8125292	100	25	25.7959184	3	0
54	119.69359	42.5955836	90.8163668	54.8174008	-35.998966	114.553772	-81.61106	-0.5593441	95.6316758	40.1813764	73.2904919	39.0972543	-34.193238	79.1495255	-78.961204	-0.6790671	93.7491519	43.2688393	75.2446031	38.9209669	-36.323636	82.1557156	-81.612129	-0.8039809	50	55	31.3779892	3	0
55	84.141073	45.6461517	73.8151459	53.4287966	-20.386349	116.42687	-97.091977	-0.6510198	129.461714	52.5199651	89.8772728	43.3163313	-46.560942	91.4753473	-118.9138	-0.672755	81.5869008	42.0551035	60.9685235	32.8982234	-28.0703	72.3043096	-69.549137	-0.7848086	50	42	25.8428334	3	0
56	69.9553498	24.6611104	53.8083807	50.9552983	-2.8530825	81.4981022	-61.557122	-0.481003	109.345477	48.0991835	82.7753008	37.390445	-45.384856	84.1530256	-92.820889	-0.725108	130.694675	39.7852892	91.4727084	46.5402007	-44.932508	75.8393248	-88.236254	-0.6645795	50	25	26.5860418	2	0
57	126.794102	50.7176408	94.2799524	64.1541358	-30.125817	124.114689	-111.3068	-0.6502036	134.37771	71.2879098	103.944842	53.5957118	-50.34913	143.183249	-144.10319	-0.7007964	81.9413769	35.5237183	61.158887	31.8332955	-29.325592	68.830854	-61.355433	-0.7254055	100	22	24.1831426	3	0
58	117.624635	67.6651783	99.2723525	80.4623704	-18.809982	117.484206	-140.30444	-0.8506391	94.4227602	70.2898959	74.7661349	37.9362774	-36.829858	146.736193	-133.34122	-0.8432911	78.9693454	51.8966126	61.4601258	33.5639845	-27.896141	86.7286817	-89.104163	-0.8708716	100	22	27.4394464	3	0
59	81.5485503	23.6144451	62.7567033	58.5065053	-4.250198	66.4553455	-53.703705	-0.5580523	83.2189662	33.1109945	72.3566228	38.3531429	-34.00348	65.2975759	-66.71465	-0.6269524	105.638815	31.6441781	72.9056144	37.2831278	-35.622487	56.0658119	-62.35257	-0.691842	100	33	22.1363224	3	0
60	86.0957076	34.0748183	79.0173027	57.1894149	-21.827888	73.2783824	-67.918029	-0.7341521	104.072755	42.7989396	74.6140276	36.3113109	-38.302717	71.8815906	-77.948782	-0.6984171	98.0199146	38.7685885	72.7770617	37.8646951	-34.912367	56.2170718	-60.029654	-0.7249523	100	34	24.748514	2	0
61	72.9145672	36.856563	61.4054497	50.8775145	-10.527935	98.1851178	-96.61829	-0.5871756	81.686453	56.2708058	61.7298016	25.0639415	-36.66586	128.513907	-113.48427	-0.7889312	86.622716	56.370531	66.9403278	31.6157919	-35.324536	99.4934173	-94.861517	-0.8714977	50	24	20.0610857	3	1
62	80.1362282	19.2326948	71.7487006	43.2767198	-28.471981	59.4762548	-62.592735	-0.3268906	140.653292	30.3677493	101.365322	46.8034479	-54.561874	78.016404	-65.101918	-0.3556086	121.425341	33.3433431	92.2549173	44.6541147	-47.600803	99.7765938	-88.731721	-0.4785384	50	24	27.4624726	3	1
63	70.780674	29.207981	55.5005416	43.5063878	-11.994154	65.2933019	-76.194468	-0.678867	59.6468051	21.8619933	43.5973028	22.3284116	-21.268891	62.1533161	-53.689109	-0.5652459	63.6916795	31.2981226	52.2443337	30.9932664	-21.251067	61.9150347	-58.917827	-0.8292712	50	23	28.9621527	3	1
64	59.0465338	22.2397491	46.7696765	31.8851244	-14.884552	56.3601281	-64.709158	-0.4485489	81.8233058	56.235949	68.0411966	34.6754139	-33.365783	128.762521	-100.0334	-0.7896542	95.2192787	40.6630372	71.4195946	35.8526945	-35.5669	80.8355622	-64.796925	-0.6346105	50	56	30.1604026	2	1
65	93.786876	12.088534	79.7849153	53.2179481	-26.566967	42.4611592	-40.082144	-0.2295136	70.8597104	13.8217901	58.6739607	29.9013544	-28.772606	35.9948294	-36.933992	-0.2807278	125.159097	13.7110568	90.7851749	48.7279076	-42.057267	27.7243475	-29.292619	-0.3133509	50	44	26.289099	3	1
66	69.0250739	14.7542018	46.8219135	29.8566756	-16.965238	47.0038258	-43.228661	-0.4841199	77.4548582	31.507061	63.9659076	33.3669181	-30.59899	67.070306	-76.339798	-0.5719741	42.9222405	21.4969485	43.0142743	21.5748668	-21.439407	48.5429896	-51.874925	-0.6485903	50	55	31.3779892	3	1
67	75.5910331	37.7955166	64.9591609	50.0668341	-14.892327	100.545502	-105.89662	-0.5813146	132.66735	57.8071243	93.6163098	45.4381539	-48.178156	113.032241	-105.27132	-0.6653594	80.8148046	37.0710113	64.4051968	34.5648829	-29.840314	66.2083956	-74.202372	-0.7146886	50	42	25.8428334	3	1
68	108.153748	42.5522941	81.2020449	63.6459822	-17.556063	111.188642	-79.400795	-0.7126059	101.967679	38.1187585	70.6010432	34.6703407	-35.930702	67.8428907	-74.516381	-0.6454469	73.9093726	31.6528362	61.635867	33.7607459	-27.875121	48.4202699	-53.531879	-0.7964406	50	25	26.5860418	2	1
69	127.328871	40.8105355	98.4761495	74.5685898	-23.90756	130.374111	-90.568963	-0.5836244	115.884145	48.4195592	91.0559935	45.1902401	-45.865753	93.5700294	-102.44734	-0.6030475	62.6965592	21.7193623	52.5967782	25.5957374	-27.001041	45.3645716	-47.559568	-0.5841373	100	22	24.1831426	3	1
70	78.0026127	41.1623286	66.3003831	53.5251773	-12.775206	104.651656	-78.595668	-0.7525838	72.8039426	41.8413463	58.7614378	26.9249249	-31.836513	96.0205544	-88.338636	-0.7010303	46.5077961	31.673868	40.7438829	22.4803893	-18.263494	59.509727	-60.340722	-0.8212254	100	22	27.4394464	3	1
71	104.339477	26.9727213	80.5237507	66.8756068	-13.648144	65.7727944	-64.919972	-0.5273207	90.5438039	22.6076914	64.94426	29.8500743	-35.094186	47.8672502	-43.88113	-0.4411637	82.6895127	18.8860707	61.1476927	32.1479721	-28.999721	34.3986883	-40.540247	-0.5074712	100	33	22.1363224	3	1
72	80.9638116	31.1999274	62.3661936	46.9131425	-15.453051	72.4589898	-52.421047	-0.6848579	107.019942	30.019619	79.7101716	39.0301585	-40.680013	60.8236504	-56.823925	-0.5081714	91.7304379	32.5477604	69.7728525	37.370869	-32.401984	52.4028762	-63.871831	-0.6806856	100	34	24.748514	2	1
73	96.2951377	63.8420802	77.3086591	54.1567564	-23.151903	127.201849	-128.72078	-0.8246169	59.3037247	37.6930454	47.6745341	21.0263382	-26.648196	84.9241906	-80.12579	-0.5107251	67.455367	59.4320414	54.4056725	23.9899834	-30.415689	98.6165311	-103.63916	-0.8922129	100	45	23.1713088	3	1
74	108.830792	53.7878709	82.9966438	65.0723863	-17.924257	104.432999	-102.65272	-0.814968	103.690416	50.2132763	80.3098914	43.1332905	-37.176601	104.199079	-109.13451	-0.6802394	84.0973351	39.3898525	64.0147795	34.5801011	-29.434678	66.1468653	-76.124334	-0.766051	100	23	21.9085299	2	1
75	141.881934	61.1560059	110.932912	92.6262648	-18.306647	133.940349	-138.27406	-0.6589073	86.679211	39.1622941	72.0096279	35.3760896	-36.633538	78.3912316	-91.701702	-0.5969525	63.3378579	32.1784206	57.6499861	30.438718	-27.211268	57.2419166	-65.923041	-0.6982757	100	25	25.7959184	3	1
76	73.8785439	45.3242601	56.9748213	49.091806	-7.8830153	115.574237	-115.39797	-0.6355405	73.7893442	60.1543567	63.4119975	26.9895711	-36.422426	128.908374	-114.78163	-0.7846542	85.8559072	62.6685454	69.6364313	31.4908065	-38.145625	106.831263	-117.09193	-0.8812571	50	24	20.0610857	3	1
77	69.2143718	21.1988888	69.3436558	51.4906176	-17.853038	65.1913819	-167.7551	-0.3147305	121.024695	26.6085807	101.134845	51.8462651	-49.288579	80.0781261	-61.662871	-0.2886187	126.344641	35.7410581	93.1006699	44.6981003	-48.40257	101.126915	-104.62306	-0.489781	50	24	27.4624726	3	1
78	61.6373542	27.9112547	54.6304969	45.1977844	-9.4327125	60.5918664	-76.335821	-0.625329	60.5179187	21.8344866	45.506888	25.4034911	-20.103397	55.1687987	-49.520866	-0.5433865	59.5814336	26.7381153	52.394997	30.8285576	-21.566439	57.5981918	-51.383825	-0.7376703	50	23	28.9621527	3	1
79	57.8463895	27.2645983	55.8215807	41.4287297	-14.392851	62.6334439	-63.254883	-0.4707422	102.256491	65.8303591	76.3104701	39.925698	-36.384772	144.190866	-141.12289	-0.7952435	84.6814688	46.3584683	71.3743371	37.9766799	-33.397657	78.6740828	-81.999926	-0.7734367	50	56	30.1604026	2	1
80	94.5587251	9.98332484	80.976037	50.6169417	-30.359095	34.4193494	-32.886146	-0.2063089	64.2125849	12.7659215	56.897989	31.14683	-25.751159	34.4716617	-35.202713	-0.3106617	108.426567	12.3282055	76.065634	40.0049728	-36.060661	26.8146436	-26.378246	-0.2890555	50	44	26.289099	3	1
81	60.3835496	22.2270735	51.8805655	35.4684267	-16.412139	50.5981686	-64.954365	-0.6248667	85.9129766	31.9973842	69.336511	39.6151814	-29.72133	65.7015329	-67.513079	-0.7096647	49.9247363	21.9932759	42.8838362	20.8735184	-22.010318	40.6356304	-41.910699	-0.8073733	50	55	31.3779892	3	1
82	73.5417972	35.1034832	64.3268584	49.5593158	-14.767543	115.755875	-72.495005	-0.5236869	114.890205	56.9233055	93.0193218	45.674662	-47.34466	106.405434	-109.93495	-0.6989705	83.4494669	37.646376	62.2414651	33.9531229	-28.288342	68.7773896	-65.894689	-0.694736	50	42	25.8428334	3	1
83	100.186551	38.6323462	77.7440896	61.5374585	-16.206631	83.6927944	-77.817242	-0.725334	102.929587	35.989366	71.8272531	35.548357	-36.278896	65.999982	-59.227571	-0.6025928	75.9014323	26.5235058	63.8441391	33.2480114	-30.596128	43.1699186	-42.882004	-0.7359942	50	25	26.5860418	2	1
84	120.95307	37.2928274	92.6162558	74.4948785	-18.121377	132.659601	-88.793922	-0.5456199	108.926486	42.2741862	82.8624437	44.136233	-38.726211	91.3805673	-91.201761	-0.528795	56.8743195	20.8585524	49.0980348	24.416644	-24.681391	50.4428486	-39.411602	-0.5511689	100	22	24.1831426	3	1
85	78.1774436	44.2931692	65.6128039	56.1806051	-9.4321988	110.907795	-86.255349	-0.7955006	63.3107489	45.2219635	60.3284869	26.6024931	-33.725994	108.123503	-95.58405	-0.7236306	41.4065535	27.2411536	33.410552	17.7593004	-15.651252	49.8617323	-57.423688	-0.7880117	100	22	27.4394464	3	1
86	104.872934	28.6799273	78.8310447	68.6692594	-10.161785	78.1467492	-72.416029	-0.504331	94.797641	23.7687357	65.1861308	30.3348499	-34.851281	44.128989	-44.309426	-0.4986686	79.8495941	19.3888128	59.8607835	32.6003596	-27.260424	38.5390367	-37.335285	-0.5428671	100	33	22.1363224	3	1
87	76.1072125	32.3630953	67.5149517	49.949226	-17.565726	71.8505514	-50.481405	-0.6369334	98.9325261	28.1992948	69.4237186	35.8600105	-33.563708	54.2863325	-54.654849	-0.5635584	90.5804682	32.4467349	69.3901298	35.8467298	-33.5434	49.6067164	-48.607002	-0.696266	100	34	24.748514	2	1
88	99.2771471	67.9205112	81.3048229	55.415665	-25.889158	147.799742	-155.00059	-0.7923515	68.2699056	50.8844017	60.6914648	28.6584507	-32.033014	95.2517906	-126.90932	-0.5340066	62.1684307	61.2496854	52.4244877	24.3088919	-28.115596	110.49602	-91.227447	-0.8819234	100	45	23.1713088	3	1
89	110.62153	58.2218577	84.5026263	68.2109125	-16.291714	112.78243	-113.0071	-0.8101302	86.5094633	43.7653271	70.0667341	36.9326537	-33.13408	83.742791	-95.723552	-0.7470161	61.223855	34.98506	56.7107443	32.4641026	-24.246642	71.7017366	-62.835292	-0.7184477	100	23	21.9085299	2	1
90	156.602361	51.3169943	121.960077	97.4770212	-24.483056	149.159964	-126.39687	-0.5971923	77.342543	40.7781422	72.636518	35.7887357	-36.847782	74.9443648	-80.826904	-0.6374979	45.9064952	19.4656517	36.676233	19.5537266	-17.122506	34.9074254	-39.808602	-0.740896	100	25	25.7959184	3	1
91	84.7833317	42.2508298	66.4638397	60.4960744	-5.9677654	97.0903622	-94.401471	-0.6520096	86.3750864	48.0306319	73.9749704	37.758968	-36.216002	118.238446	-125.24331	-0.6581069	87.2664897	32.3608738	66.6018867	31.4155552	-35.186331	62.7709249	-64.867292	-0.6140832	50	44	38.9042275	2	1
92	62.9135098	32.2633384	59.045253	48.758001	-10.287252	103.800222	-66.829742	-0.4101146	95.8532295	28.669959	71.4347894	31.7046985	-39.730091	72.0248998	-73.838609	-0.4810788	115.434014	56.3550924	92.0813686	46.6241957	-45.457173	108.195326	-108.8307	-0.6555029	50	27	20.0150311	3	1
93	88.1827072	39.3965929	59.2890684	62.3839278	3.09485932	133.245511	-129.69314	-0.5047465	57.056984	38.250492	52.1597188	20.2672269	-31.892492	95.0327443	-82.068964	-0.6835393	93.1200613	45.6470889	62.587291	36.8391695	-25.748121	81.2970848	-99.598276	-0.6397599	50	65	42.8187176	2	1
94	57.2480038	24.6738167	48.1063657	38.1956751	-9.9106906	65.3216826	-57.449923	-0.3996091	51.7404064	24.2343824	45.4089232	20.2594985	-25.149425	57.0089824	-56.470641	-0.5641175	55.3293263	22.4459742	46.1274363	26.5542489	-19.573187	46.1927968	-54.836892	-0.5799666	50	29	25.4680385	2	1
95	76.7522838	40.3251929	65.2654527	55.2136193	-10.051833	80.073433	-108.52869	-0.6425516	110.273934	58.6043939	84.5555632	41.6455246	-42.910039	123.542122	-130.49251	-0.6466519	69.0802924	39.5875601	56.8646467	25.9051096	-30.959537	72.7496436	-68.591459	-0.724374	50	60	33.1391536	1	1
96	72.5987051	32.2422081	63.128977	49.0548284	-14.074149	65.3147951	-73.821667	-0.7148091	93.7748559	42.7870065	70.2933867	32.7707631	-37.522624	88.0249584	-90.317618	-0.7116198	69.8303163	30.4050724	57.24714	27.7236672	-29.523473	64.0062824	-63.872953	-0.7649722	50	52	25.9181378	1	1
97	83.5998495	27.1134647	72.3594753	64.0879817	-8.2714936	50.2543972	-64.109781	-0.6052681	57.3562615	16.2635902	49.876405	22.3317058	-27.544699	37.7776021	-40.909755	-0.5273823	84.7091347	23.8393437	64.3657334	33.6480716	-30.717662	40.1638291	-45.16462	-0.6587694	50	41	20.8984375	2	1
98	105.341338	36.2620785	107.874561	65.2827648	-42.591796	83.1157822	-70.948851	-0.4972375	109.080714	29.7087738	83.6242911	39.4291677	-44.195123	68.2756358	-72.024546	-0.4313163	99.4791681	31.6141424	73.3781785	35.1397005	-38.238478	58.8525005	-65.383044	-0.6963003	50	28	26.9382125	3	1
99	82.9340003	32.6297706	66.8516925	49.8006369	-17.051056	105.605736	-98.060737	-0.4411346	68.5964732	28.2096531	59.4116009	29.4361949	-29.975406	62.4292269	-57.094473	-0.5316683	93.4645317	36.2969055	67.1228147	35.8913283	-31.231486	80.6621735	-84.310466	-0.6512949	100	45	27.4576145	2	1
100	87.4358349	40.2930115	75.4349967	61.8302229	-13.604774	152.079171	-99.530196	-0.5354428	83.3951758	21.3014498	69.8712545	34.9113052	-34.959949	51.8979349	-53.654317	-0.4065934	57.5946903	26.9764357	56.3500437	32.0032238	-24.34682	60.0387023	-65.418233	-0.496763	100	56	28.5289346	2	1

Figure 1: Complete table after filtration and data transformation.

.2 Annex: Weka ranking of variable predictive capabilities

```
=== Run information ===

Evaluator:     weka.attributeSelection.ClassifierAttributeEval DEFAULT --
Search:        weka.attributeSelection.Ranker -T -1.7976931348623157E308 -N -1
Instances:     150
Attributes:    26
               Rx.01.Length.10
               Rx.02.Vel
               Rx.03.MaxRange
               Rx.05.Max
               Rx.10.Min
               Rx.15.Speed.Max
               Rx.20.Speed.Min
               Ry.01.Length.10
               Ry.02.Vel
               Ry.03.MaxRange
               Ry.05.Max
               Ry.10.Min
               Ry.15.Speed.Max
               Ry.20.Speed.Min
               Rz.01.Length.10
               Rz.02.Vel
               Rz.03.MaxRange
               Rz.05.Max
               Rz.10.Min
               Rz.15.Speed.Max
               Rz.20.Speed.Min
               Sexo
               Edad
               Nivel Estudios
               BMI2
               Estado
Evaluation mode:    evaluate on all training data
```

```
=== Attribute Selection on all input data ===

Search Method:
Attribute ranking.

Attribute Evaluator (supervised, Class (nominal): 26 Estado):Classifier
feature evaluator

Using  Wrapper Subset Evaluator
Learning scheme: weka.classifiers.rules.ZeroR
Scheme options:
Subset evaluation: classification accuracy
Number of folds for accuracy estimation: 5


Ranked attributes:
  0   25 BMI2
  0   12 Ry.10.Min
  0    8 Ry.01.Length.10
  0    9 Ry.02.Vel
  0   10 Ry.03.MaxRange
  0    7 Rx.20.Speed.Min
  0    6 Rx.15.Speed.Max
  0    5 Rx.10.Min
  0    2 Rx.02.Vel
  0    3 Rx.03.MaxRange
  0    4 Rx.05.Max
  0   11 Ry.05.Max
  0   13 Ry.15.Speed.Max
  0   24 Nivel Estudios
  0   14 Ry.20.Speed.Min
  0   21 Rz.20.Speed.Min
  0   22 Sexo
  0   23 Edad
  0   20 Rz.15.Speed.Max
  0   19 Rz.10.Min
```

0 18 Rz.05.Max
0 15 Rz.01.Length.10
0 16 Rz.02.Vel
0 17 Rz.03.MaxRange
0 1 Rx.01.Length.10

Selected attributes: 25,12,8,9,10,7,6,5,2,3,4,11,13,24,14,2//
1,22,23,20,19,18,15,16,17,1 : 25

.3 Annex: Revision and correction of the curves generate with the MoveHuman interface

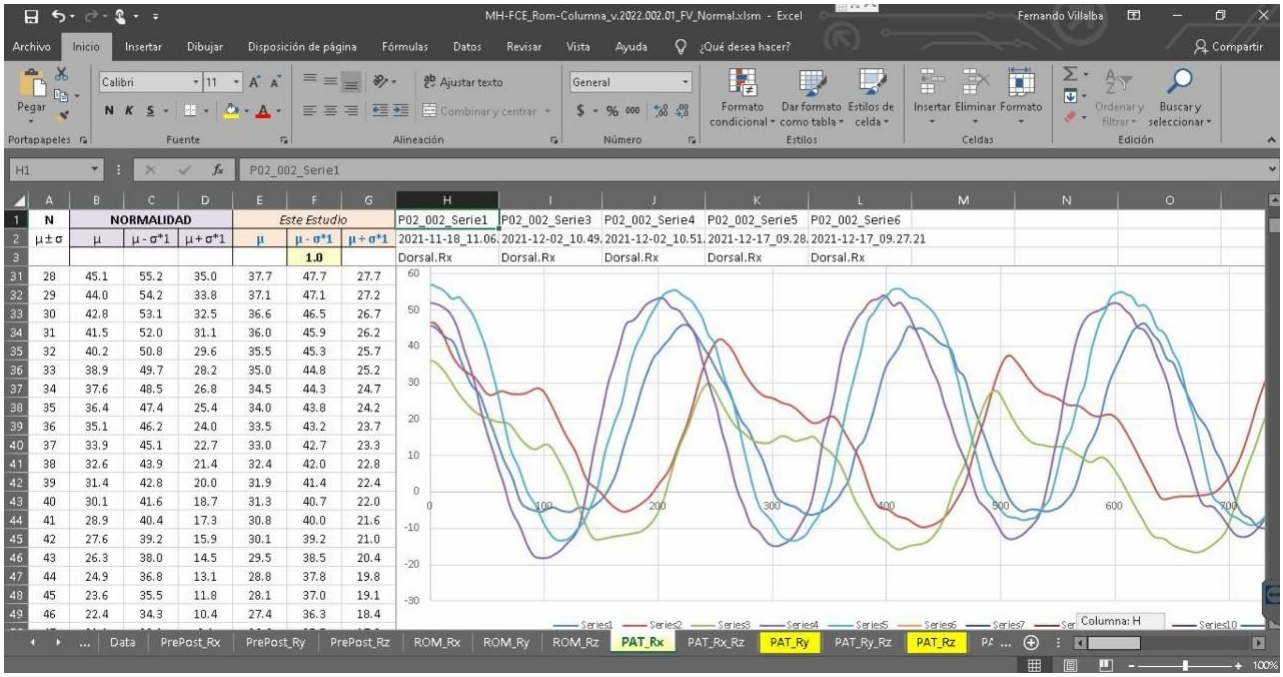

Figure 2: Evaluation and analysis of curves generated using angular changes.

.4 Annex: Reports generated with the MoveHuman software

PRUEBA DE BIOMECÁNICA DE COLUMNA LUMBAR Y DORSAL

Fecha
02 de mayo de 2023

Prueba desarrollada por el grupo de investigación IDERGO (Investigación y desarrollo en ergonomía)
Universidad de Zaragoza.

http://idergo.unizar.es/

v.19-07.011

ÍNDICE

1. MÉTODO Y VALORACIÓN DE LA COLUMNA CERVICAL.

1.1 OBJETO DE LA PRUEBA.

La prueba de valoración de la columna lumbar y dorsal se realiza con el propósito de valorar la capacidad funcional de la columna, así como la consistencia en la ejecución de la misma. En esta prueba se trata de objetivar alteraciones de la movilidad articular del paciente. En concreto se valorará su capacidad funcional en relación a los datos de referencia de una muestra de individuos sanos analizada, así como el grado de colaboración que ha mostrado durante la prueba.

1.2 TECNOLOGÍA.

El método utilizado se basa en la captura del movimiento mediante un sistema de análisis tridimensional del movimiento (*Move*Human-Sensors ©UZ) basado en sensores inerciales que se fijan en las zonas corporales a evaluar. En este caso se fijan sensores en la zona pélvica (sacro) y dorsal (D2). Se utiliza el sistema de referencia de la fig 1.

Fig 1. Sistema de referencia

1.3 MOVIMIENTOS ANALIZADOS.

Los movimientos que se analizan en la columna lumbar y dorsal son los siguientes (fig.2):

- **Flexión-extensión (Rx).** Corresponde al movimiento de la columna en el plano sagital. La flexión es un movimiento hacia adelante desde la posición neutra del tronco (valor positivo) y la extensión un movimiento hacia atrás desde esa misma posición (valor negativo). Se le denomina rotación eje X (Rx).
- **Rotación (Ry)**. Corresponde a una rotación en un eje vertical al suelo. Tendremos rotación hacia la derecha (valor positivo) y hacia la izquierda (valor negativo). Es una rotación en el eje Y (Ry).
- **Inclinación (Rz)**. Corresponde a un movimiento en el plano frontal. Tendremos lateralización derecha (valor positivo) e izquierda (valor negativo). Es una rotación en el eje Z (Rz).

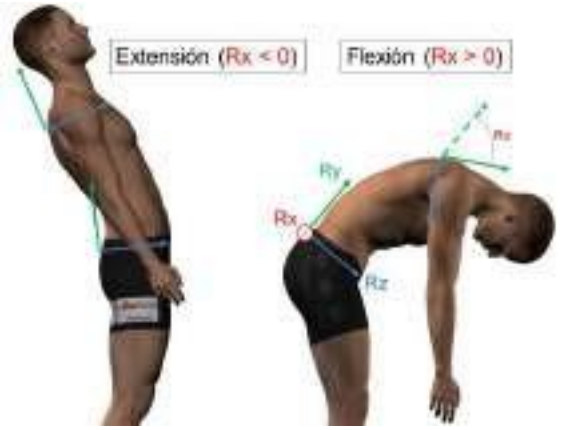

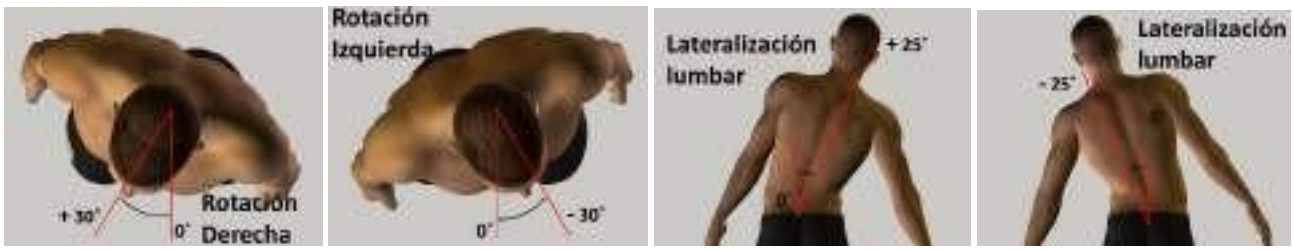

Fig 2. Ángulos analizados en la columna cervical.

1.4 METODOLOGÍA.

La prueba del rango articular (ROM) de columna consiste en realizar una captura para cada uno de los movimientos indicados: flexión-extensión, rotación y lateralización. En cada captura el paciente debe llegar a repetir un total de 7 ciclos de movimientos completos tratando de llegar a su máximo rango en cada ciclo y procurando mantener una velocidad de movimiento lo más uniforme posible. Previo a cada captura se llevan a cabo unos ejercicios de calentamiento y se instruye al sujeto por medio de unos videos que muestran cómo realizar cada ejercicio, con la finalidad de que pueda realizar los movimientos varias veces a modo de prueba. La posición neutra de la columna (Rx=0; Ry=0; Rz=0) se calibra al comienzo de cada prueba; para ello se pide al sujeto que se coloque mirando al frente en posición relajada.

1.5 ANÁLISIS DE DATOS: DESCRIPCIÓN DE RESULTADOS.

El procesado de datos de la captura permite analizar los movimientos relativos del sensor ubicado en D2 respecto al fijado en la región del sacro. El valor de los ángulos resultantes de la captura, da lugar a diferentes gráficos y tablas con parámetros. Cada movimiento capturado (flexión-extensión, rotación y lateralización) se divide en tres apartados: (1) ángulos, (2) velocidades y (3) aceleraciones. La estructura de datos se mantiene para todos los movimientos capturados; por ello se expone únicamente la descripción de gráficos y parámetros resultantes del movimiento de Flexión-extensión (Rx), pero es equivalente para la rotación (Ry) y para la lateralización (Rz).

1.5.1 ÁNGULOS.

Los resultados angulares constan de dos gráficos; el primero representa la variación del ángulo en grados a lo largo del tiempo Rx (Flexión-extensión), asimismo se representa los movimientos acoplados, en este caso, Rz (lateralización) y Ry (Rotación). El tiempo se presenta en fotogramas o frames, se puede utilizar la frecuencia de captura (fps), que incluye el informe, para hacer la transformación. El segundo gráfico muestra los distintos ciclos de flexión y extensión realizados, pero superpuestos, de esta forma se puede apreciar la regularidad de los mismos en cuanto a la longitud de los ciclos en segundos y a la amplitud en grados.

Los parámetros angulares resultantes son los siguientes:

Nombre	**Definición**
Rx.Length	Grados totales recorridos durante la ejecución del movimiento
Rx.Vel	Velocidad angular promedio. Cociente entre total de grados recorridos y tiempo invertido
Rx.MaxRange	Rango total del movimiento. Suma del máximo (flexión) y mínimo (extensión) alcanzado.
Rx.Max	Valor máximo de ángulo en el movimiento de flexión.
Rx.MaxMean	Valor medio de los 5 máximos alcanzados en el movimiento de flexión.
Rx.MaxStd	Desviación estándar de los 5 máximos alcanzados en el movimiento de flexión.
Rx.MaxCV[%]	Coeficiente de variación del movimiento de flexión: (Rx.MaxStd / Rx.MaxMean)*100
Rx.Min	Y siguientes campos, mismo significado para el movimiento de extensión

Para cada uno de los citados parámetros se recoge en la tabla el **valor** alcanzado por el paciente durante el movimiento; los **valores de referencia** de una muestra de sujetos sanos (límite inferior, valor medio y límite superior); los límites se calculan sumando y restando al valor medio dos veces la desviación estándar; y la **valoración de la diferencia** entre el valor del paciente y los datos de referencia de acuerdo a las siguientes consideraciones:

- Para los parámetros de desviación estándar y coeficiente de variación, la valoración es la siguiente:
  - **En rango**, cuando el valor del paciente sea inferior o igual al límite superior de referencia.
  - **Fuera de rango**, cuando el valor del paciente sea superior al límite superior de la muestra.

- Para el resto de parámetros la valoración es la siguiente:
  - Si el valor del paciente es superior o igual al valor medio de referencia, mostrará el % de incremento respecto a la normalidad e indicará **capacidad (OK)**.
  - Si el valor del paciente se encuentra entre el límite inferior y superior, mostrará el % de reducción respecto a la normalidad e indicará **capacidad (en rango)**.
  - Si el valor del paciente está por debajo del límite inferior de referencia, mostrará el % de reducción e indicará **capacidad (a valorar)**.

Como información complementaria se aportan los ángulos acoplados, en este caso (Rx) y (Ry), durante los rangos de movimiento máximos (flexión) o mínimos (extensión), indicando en los instantes o fotogramas donde se han alcanzado. Se utiliza la siguiente terminología y estructura:

Cervical.Rx.MaxPeaks: [Primer máximo Rx, Acoplado Rz, Acoplado Ry, Frame] [Segundo máximo Rx, …]

Por último, se incluye los fotogramas correspondientes a los instantes donde se ha obtenido los máximos valores de flexión y extensión.

1.5.2 VELOCIDADES

Los resultados de velocidad constan de dos gráficos; el primero muestra en línea continua la velocidad angular en grados por segundo a lo largo del tiempo (frames o fotogramas de captura), y en línea discontinua el valor del ángulo de rotación (Rx de flexión-extensión) en cada instante. El segundo gráfico muestra el valor de la velocidad angular (eje de ordenadas) respecto al ángulo de rotación (eje de abscisas) alcanzado en cada instante; cada bucle representa un ciclo de movimiento.

Los parámetros relativos a la velocidad se describen en la siguiente tabla, destacar que la valoración de los resultados (en rango, fuera de rango, etc.) se estructura de la mismo forma que el apartado de ángulos.

Nombre	Definición
Rx.Speed.Max	Valor máximo de la velocidad en el movimiento de flexión.
Rx.Speed.MaxMean	Valor medio de los 5 máximos de velocidad alcanzados en el movimiento de flexión.
Rx.Speed.MaxStd	Desviación estándar de los 5 máximos alcanzados en el movimiento de flexión.
Rx.Speed.MaxCV[%]	Coeficiente de variación del movimiento de flexión.
Rx.Speed.Min	Y siguientes, mismo significado para el movimiento de extensión.
Rx.Speed.AreaMean	Área de movilidad. Área media del gráfico ángulo-velocidad angular.
Rx.Speed.AreaStd	Área de variabilidad. Área encerrada por las curvas de desviación estándar del gráfico ángulo-velocidad angular.
Rx.Speed.AreaCoef[%]	Variabilidad relativa. Cociente entre áreas de variabilidad y movilidad.

Como información complementaria, se incluye el valor del ángulo de flexión (Rx) durante a los instantes (frames) de máxima velocidad. Se utiliza la siguiente terminología y estructura:

Cervical.Rx.Speed.MaxPeaks: [Primera velocidad máxima, Ángulo (Rx), Frame] [Segunda velocidad, …]

1.5.3 ACELERACIONES.

Los resultados de velocidad incluyen dos gráficos; el primero muestra en línea continua la aceleración angular en grados al cuadrado por segundo a lo largo del tiempo (frames o fotogramas de captura), y en línea discontinua el valor del ángulo de rotación (Rx de flexión-extensión) en cada instante. El segundo gráfico muestra el valor de la aceleración angular (eje de ordenadas) respecto al ángulo de rotación (eje de abscisas) alcanzado en cada instante; cada línea representa un ciclo de movimiento.

Los parámetros relativos a las aceleraciones se describen en la siguiente tabla, destacar que la valoración de los resultados (en rango, fuera de rango, etc.) se estructura de la mismo forma que el apartado de ángulos.

Nombre	Definición
Rx.SpeedUp.Max	Valor máximo de la aceleración en el movimiento de flexión.
Rx.SpeedUp.MaxMean	Valor medio de los 5 máximos de aceleración en el movimiento de flexión.
Rx.SpeedUp.MaxStd	Desviación estándar de los 5 máximos alcanzados en el movimiento de flexión.
Rx.SpeedUp.MaxCV[%]	Coeficiente de variación del movimiento de flexión.
Rx.SpeedUp.Min	Y siguientes, mismo significado para el movimiento de extensión
Rx.SpeedUp.Harmony	Armonía. Coeficiente de correlación de Pearson entre ángulo y aceleración angular. Linealidad del gráfico ángulo-velocidad angular Valor ideal de movimiento armónico simple = -1
Rx.SpeedUp.Offset[deg]	Desfase. Diferencia media de fases entre las ondas (ciclos de movimiento). Valor ideal de movimiento armónico simple = 180)

Como información complementaria, se incluye el valor del ángulo de flexión (Rx) durante a los instantes (frames) de máxima aceleración. Se utiliza la siguiente terminología y estructura:

Cervical.Rx.SpeedUp.MaxPeaks: [1ª aceleración máxima, Ángulo (Rx), Frame] [2ª aceleración máxima, ...]

2. DATOS DE IDENTIFICACIÓN

ID sujeto: 022
ID operador: 001
Motivo Prueba:

Capture date: 2021-08-06_12.42.47 fps: 60
MoveHuman v.2021-08.091.18

ID sujeto: '022'

3. VALORACIÓN Y CONCLUSIONES.

En las siguientes páginas se recoge los resultados de las pruebas llevadas a cabo sobre el paciente, relativas a la evaluación funcional de la articulación indicada y siguiendo la metodología expuesta previamente.

Las conclusiones más relevantes que se desprenden del análisis de dichos resultados son las siguientes:

-

-

La ejecución del movimiento fue homogénea/no homogénea y su consistencia adecuada/inadecuada.

Los resultados obtenidos deben ser contrastados con las lesiones sufridas y valorados en el contexto de la historia clínica del sujeto.

Fdo: _____

ID sujeto: '022'

4. DATOS DE LA CAPTURA: 01S1.COLUMNA.FLEX

4.1 Resultados: 01s1.Columna.Flex - Dorsal.Rx

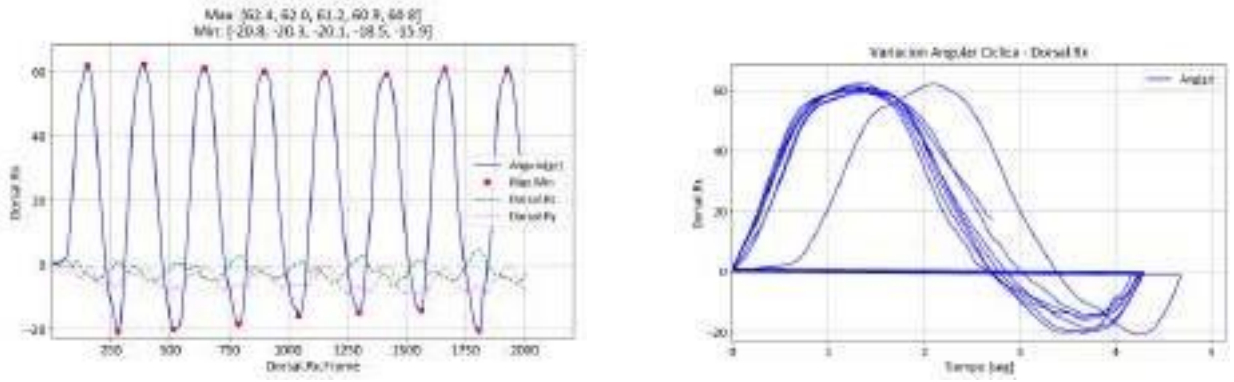

Fig 3. Gráfico Dorsal.Rx

Units: Rot[gr] Trans[cm]

Columna.Flex	*Valor captura*	*Valores Referencia*	*Diferencia %*
Rx.Length.10	110.0	[65, 118, 171]	-7 % (en rango)
Rx.Vel	37.2	[10, 27, 44]	38 % (ok)
Rx.MaxRange	83.2	[67, 105, 143]	-21 % (en rango)
Rx.Max	62.4	[45, 74, 104]	-16 % (en rango)
Rx.MaxMean	61.5	[43, 72, 102]	-15 % (en rango)
Rx.MaxStd	0.7	[0, 1.8, 3.6]	En rango
Rx.MaxCV[%]	1.2	[0, 2.4, 5.4]	En rango
Rx.Min	-20.8	[-13, -32, -52]	-37 % (en rango)
Rx.MinMean	-19.1	[-9, -29, -48]	-34 % (en rango)
Rx.MinStd	2.0	[0.4, 3.3, 6.3]	En rango
Rx.MinCV[%]	-10.6	[0, -12.3, -28.4]	En rango

[Dorsal.Rx, Acoplados: ['Dorsal.Rz', 'Dorsal.Ry'], Frame]

Dorsal.Rx.MaxPeaks: [62.4, -3.5, -1.2, 388] [62.0, -2.9, -1.0, 151] [61.2, -3.9, -0.3, 644] [60.9, -3.8, -1.0, 1662] [60.8, -3.6, 0.1, 1928]

Dorsal.Rx.MinPeaks: [-20.8, 1.0, -6.3, 280] [-20.3, 4.2, -7.0, 1807] [-20.1, -0.0, -7.4, 514] [-18.5, 2.6, -5.9, 788] [-15.9, 0.6, -6.4, 1044]

Fig 4. Dorsal.Rx. Max: array([62.39, -3.53, -1.2 , 388.]). Min: array([-20.82, 0.99, -6.34, 280.])

Capture: 01s1.Columna.Flex. 2021-08-06_12.42.47 Operador: '001' IDsujeto: '022'

4.2 Resultados: 01s1.Columna.Flex - Dorsal.Rx.Speed

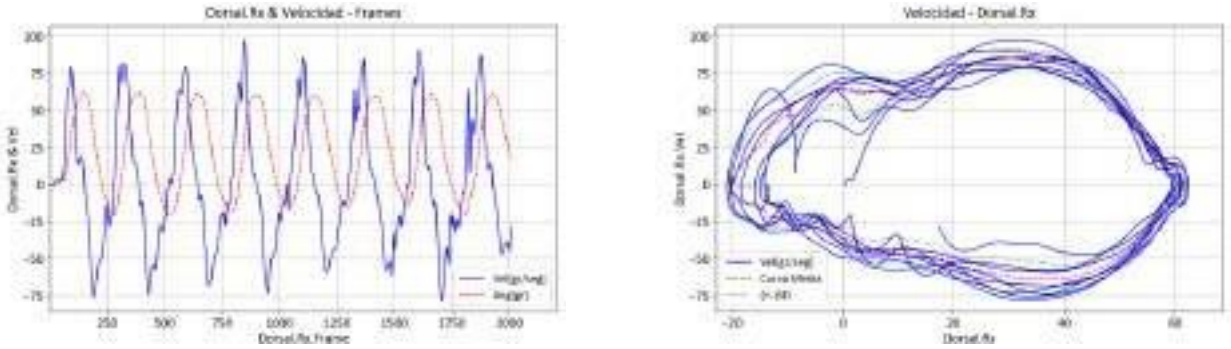

Fig 5. Gráficos Velocidad Angular

Units: Rot[gr/seg] Trans[cm/seg]

Columna.Flex	*Valor captura*	*Valores Referencia*	*Diferencia %*
Rx.Speed.Max	97.5	[37, 91, 144]	8 % (ok)
Rx.Speed.MaxMean	89.2	[31, 78, 126]	14 % (ok)
Rx.Speed.MaxStd	5.2	[0, 10, 19]	En rango
Rx.Speed.MaxCV[%]	5.8	[0, 11, 24]	En rango
Rx.Speed.Min	-78.0	[-41, -84, -126]	-7 % (en rango)
Rx.Speed.MinMean	-73.8	[-34, -73, -112]	1 % (ok)
Rx.Speed.MinStd	3.7	[0, 9, 19]	En rango
Rx.Speed.MinCV[%]	-5.0	[0, -11, -25]	En rango
Rx.Speed.AreaMean	165.7	[22, 143, 263]	17 % (ok)
Rx.Speed.AreaStd	52.5	[19, 130, 240]	En rango
Rx.Speed.AreaCoef[%]	31.7	[0, 107, 233]	-73 % (en rango)

Dorsal.Rx.Speed.MaxPeaks[Val,Ang,fr]: [97.5, 31.4, 849] [90.7, 26.5, 1607] [87.2, 35.4, 1878] [85.8, 28.4, 1103] [84.7, 39.6, 1368]

Dorsal.Rx.Speed.MinPeaks[Val,Ang,fr]: [-78.0, 33.1, 1708] [-75.6, 34.4, 193] [-74.0, 37.3, 431] [-73.2, 31.5, 950] [-68.0, 37.3, 692]

4.3 Resultados: 01s1.Columna.Flex - Dorsal.Rx.SpeedUp

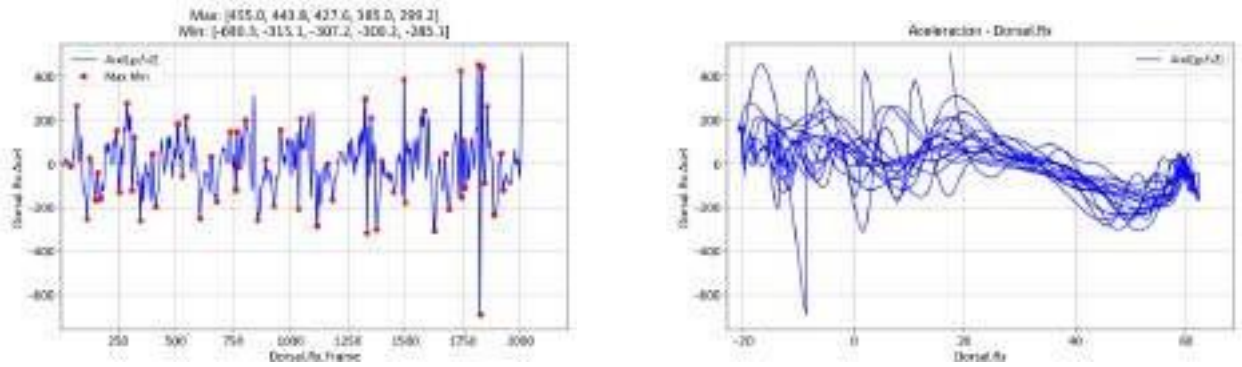

Fig 6. Gráfico Aceleración Angular

Units: Rot[gr/seg2] Trans[cm/seg2]

Columna.Flex	*Valor captura*	*Valores Referencia*	*Diferencia %*
Rx.SpeedUp.Max	455.0	[143, 409, 675]	11 % (ok)
Rx.SpeedUp.MaxMean	402.1	[127, 317, 507]	27 % (ok)
Rx.SpeedUp.MaxStd	63.4	[0, 75, 162]	En rango
Rx.SpeedUp.MaxCV[%]	15.8	[0, 20, 44]	En rango
Rx.SpeedUp.Min	-690.28	[-110, -457, -804]	51 % (ok)
Rx.SpeedUp.MinMean	-379.6	[-109, -331, -553]	15 % (ok)
Rx.SpeedUp.MinStd	174.0	[0, 106, 245]	En rango
Rx.SpeedUp.MinCV[%]	-45.9	[0, -26, -67]	En rango
Rx.SpeedUp.Harmony	-0.57	[-0.14, -0.37, -0.6]	54 % (ok)
Rx.SpeedUp.Offset[deg]	116.9	[95, 108, 121]	8 % (ok)

Dorsal.Rx.SpeedUp.MaxPeaks[Val,Ang,fr]: [455.0, -16.6, 1819] [443.8, -7.6, 1834] [427.6, 2.1, 1741] [385.0, 11.0, 1494] [299.2, -5.7, 1325]

Dorsal.Rx.SpeedUp.MinPeaks[Val,Ang,fr]: [-690.3, -8.6, 1827] [-315.1, 1.7, 1332] [-307.2, 51.7, 1626] [-300.2, 47.4, 1374] [-285.1, 45.7, 1116]

ID sujeto: '022'

5. DATOS DE LA CAPTURA: 02S1.COLUMNA.ROT

5.1 Resultados: 02s1.Columna.Rot - Dorsal.Ry

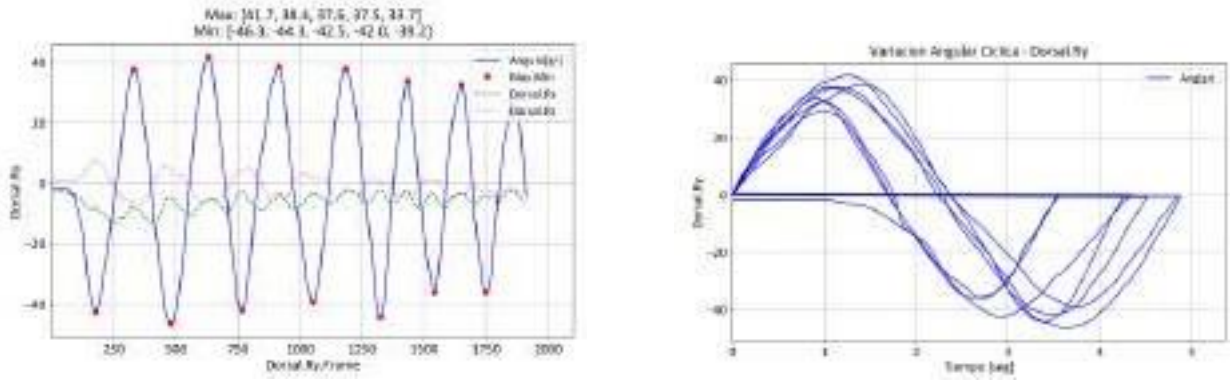

Fig 7. Gráfico Dorsal.Ry

Units: Rot[gr] Trans[cm]

Columna.Rot	*Valor captura*	*Valores Referencia*	*Diferencia %*
Ry.Length.10	93.7	[76, 115, 154]	-18 % (en rango)
Ry.Vel	35.8	[17, 43, 70]	-17 % (en rango)
Ry.MaxRange	88.0	[75, 104, 132]	-15 % (en rango)
Ry.Max	41.7	[36, 53, 69]	-20 % (en rango)
Ry.MaxMean	37.8	[35, 51, 67]	-26 % (en rango)
Ry.MaxStd	2.8	[0, 1.4, 2.9]	En rango
Ry.MaxCV[%]	7.5	[0, 2.3, 5.3]	A valorar
Ry.Min	-46.3	[-35, -51, -67]	-9 % (en rango)
Ry.MinMean	-42.9	[-34, -50, -65]	-14 % (en rango)
Ry.MinStd	2.7	[0.1, 1.3, 2.6]	A valorar
Ry.MinCV[%]	-6.2	[0, -2.3, -4.6]	A valorar

[Dorsal.Ry, Acoplados: ['Dorsal.Rx', 'Dorsal.Rz'], Frame]

Dorsal.Ry.MaxPeaks: [41.7, -5.2, -5.7, 631] [38.4, -4.0, -3.6, 913] [37.6, -2.3, -2.6, 1183] [37.5, -8.3, -6.7, 331] [33.7, -2.3, -4.4, 1432]

Dorsal.Ry.MinPeaks: [-46.3, -4.8, 4.1, 479] [-44.3, -2.4, 0.2, 1323] [-42.5, -8.0, 7.6, 176] [-42.0, -2.9, 4.5, 765] [-39.2, -3.2, 2.0, 1052]

Fig 8. Dorsal.Ry. Max: array([41.71, -5.19, -5.73, 631.]). Min: array([-46.32, -4.76, 4.11, 479.])

Capture: 02s1.Columna.Rot. 2021-08-06_12.53.47 Operador: '001' IDsujeto: '022'

5.2 Resultados: 02s1.Columna.Rot - Dorsal.Ry.Speed

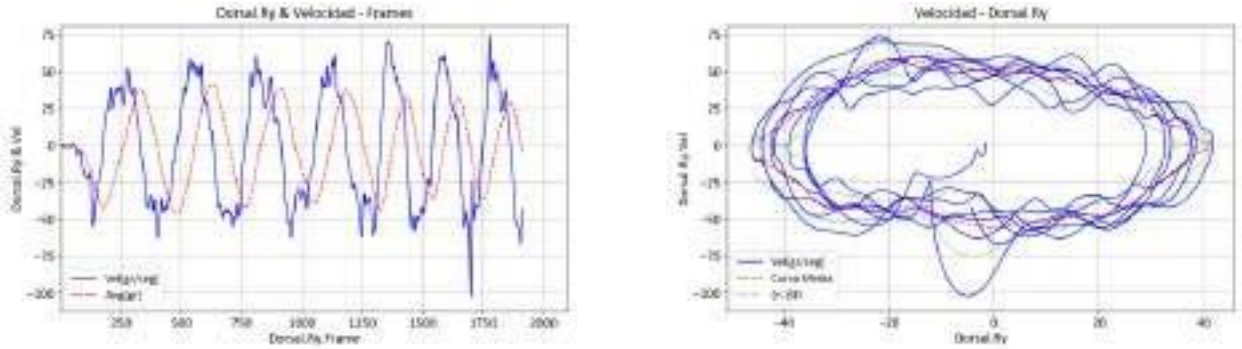

Fig 9. Gráficos Velocidad Angular

Units: Rot[gr/seg] Trans[cm/seg]

Columna.Rot	*Valor captura*	*Valores Referencia*	*Diferencia %*
Ry.Speed.Max	73.7	[46, 104, 162]	-29 % (en rango)
Ry.Speed.MaxMean	65.3	[46, 92, 137]	-28 % (en rango)
Ry.Speed.MaxStd	6.3	[0, 10, 21]	En rango
Ry.Speed.MaxCV[%]	9.7	[0, 9, 18]	En rango
Ry.Speed.Min	-102.3	[-51, -102, -153]	0 % (ok)
Ry.Speed.MinMean	-70.1	[-45, -90, -135]	-22 % (en rango)
Ry.Speed.MinStd	18.0	[0, 10, 19]	En rango
Ry.Speed.MinCV[%]	-25.7	[0, -10, -20]	A valorar
Ry.Speed.AreaMean	135.2	[52, 237, 422]	-43 % (en rango)
Ry.Speed.AreaStd	68.5	[22, 95, 168]	En rango
Ry.Speed.AreaCoef[%]	50.7	[0, 45, 93]	10 % (ok)

Dorsal.Ry.Speed.MaxPeaks[Val,Ang,fr]: [73.7, -22.0, 1778] [70.5, -21.4, 1356] [61.3, 14.5, 1135] [60.9, 2.7, 1592] [60.2, -14.7, 811]

Dorsal.Ry.Speed.MinPeaks[Val,Ang,fr]: [-102.3, -4.9, 1698] [-62.9, -2.9, 402] [-62.8, 13.0, 955] [-62.0, 6.4, 1247] [-60.7, -27.0, 1294]

5.3 Resultados: 02s1.Columna.Rot - Dorsal.Ry.SpeedUp

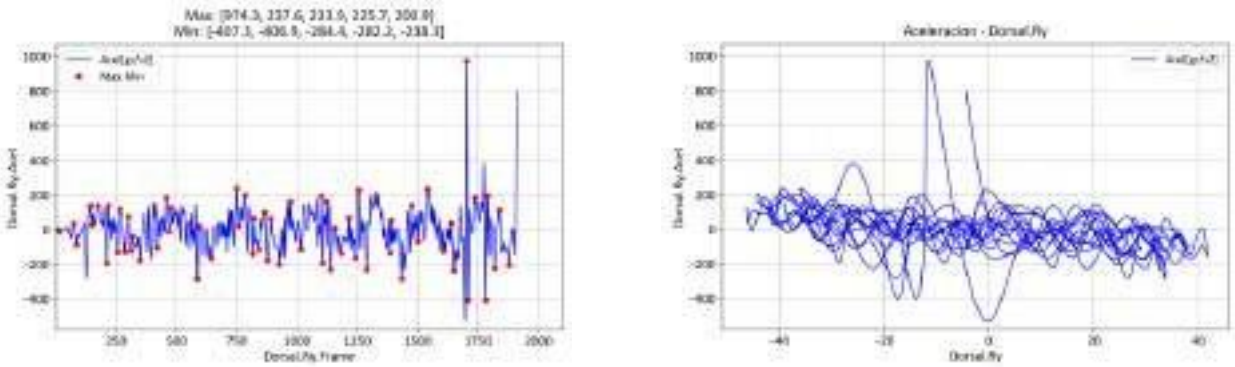

Fig 10. Gráfico Aceleración Angular

Units: Rot[gr/seg2] Trans[cm/seg2]

Columna.Rot	*Valor captura*	*Valores Referencia*	*Diferencia %*
Ry.SpeedUp.Max	974.3	[45, 500, 956]	95 % (ok)
Ry.SpeedUp.MaxMean	374.5	[132, 369, 607]	1 % (ok)
Ry.SpeedUp.MaxStd	335.6	[0, 111, 257]	A valorar
Ry.SpeedUp.MaxCV[%]	89.6	[0, 21, 48]	A valorar
Ry.SpeedUp.Min	-407.34	[-130, -487, -843]	-16 % (en rango)
Ry.SpeedUp.MinMean	-323.8	[-135, -365, -595]	-11 % (en rango)
Ry.SpeedUp.MinStd	78.2	[0, 98, 217]	En rango
Ry.SpeedUp.MinCV[%]	-24.2	[0, -21, -48]	En rango
Ry.SpeedUp.Harmony	-0.49	-	-
Ry.SpeedUp.Offset[deg]	119.4	[105, 123, 140]	-2 % (en rango)

Dorsal.Ry.SpeedUp.MaxPeaks[Val,Ang,fr]: [974.3, -11.3, 1702] [237.6, -39.4, 750] [233.9, -36.1, 1540] [225.7, -0.1, 1254] [200.9, -44.1, 1326]

Dorsal.Ry.SpeedUp.MinPeaks[Val,Ang,fr]: [-407.3, -13.9, 1709] [-406.9, -17.3, 1782] [-284.4, 33.6, 1433] [-282.2, 26.3, 587] [-238.3, 32.6, 1650]

ID sujeto: '022'

6. DATOS DE LA CAPTURA: 03S1.COLUMNA.LAT

6.1 Resultados: 03s1.Columna.Lat - Dorsal.Rz

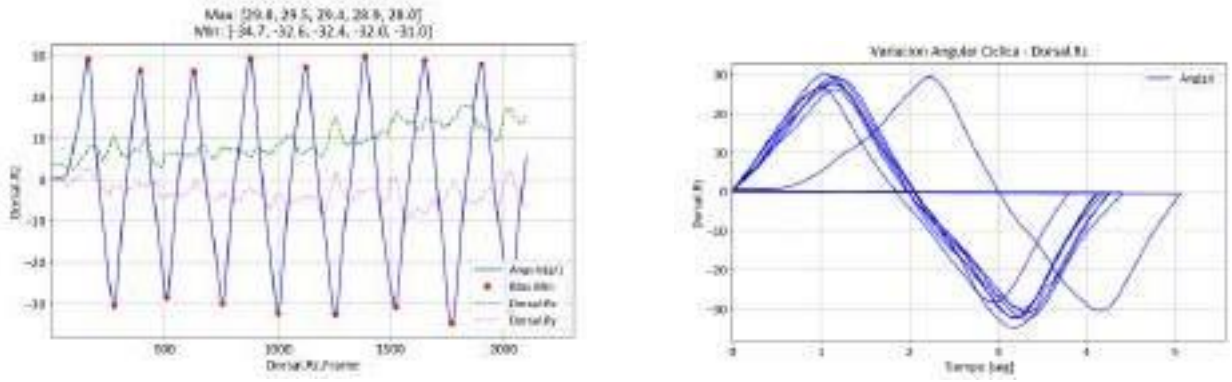

Fig 11. Gráfico Dorsal.Rz

Units: Rot[gr] Trans[cm]

Columna.Lat	*Valor captura*	*Valores Referencia*	*Diferencia %*
Rz.Length.10	89.3	[62, 102, 142]	-12 % (en rango)
Rz.Vel	28.7	[17, 35, 53]	-18 % (en rango)
Rz.MaxRange	64.6	[60, 92, 124]	-30 % (en rango)
Rz.Max	29.8	[26, 45, 63]	-32 % (en rango)
Rz.MaxMean	29.1	[25, 43, 61]	-32 % (en rango)
Rz.MaxStd	0.7	[0.4, 1.4, 2.4]	En rango
Rz.MaxCV[%]	2.5	[0.6, 3.1, 5.7]	En rango
Rz.Min	-34.7	[-31, -48, -65]	-28 % (en rango)
Rz.MinMean	-32.5	[-29, -46, -63]	-29 % (en rango)
Rz.MinStd	1.4	[0.2, 1.4, 2.7]	En rango
Rz.MinCV[%]	-4.2	[-0.2, -2.9, -5.7]	En rango

[Dorsal.Rz, Acoplados: ['Dorsal.Rx', 'Dorsal.Ry'], Frame]

Dorsal.Rz.MaxPeaks: [29.8, 9.6, -2.6, 1386] [29.5, 5.7, -1.8, 878] [29.4, 7.7, 2.7, 160] [28.9, 14.5, -8.4, 1652] [28.0, 13.5, -5.1, 1903]

Dorsal.Rz.MinPeaks: [-34.7, 14.3, -1.6, 1771] [-32.6, 15.2, 1.7, 1256] [-32.4, 8.4, -3.7, 1001] [-32.0, 17.2, 1.9, 2027] [-31.0, 16.1, 0.2, 1523]

Fig 12. Dorsal.Rz. Max: array([29.84, 9.62, -2.55, 1386.]). Min: array([-34.72, 14.29, -1.62, 1771.])

Capture: 03s1.Columna.Lat. 2021-08-06_12.48.14 Operador: '001' IDsujeto: '022'

6.2 Resultados: 03s1.Columna.Lat - Dorsal.Rz.Speed

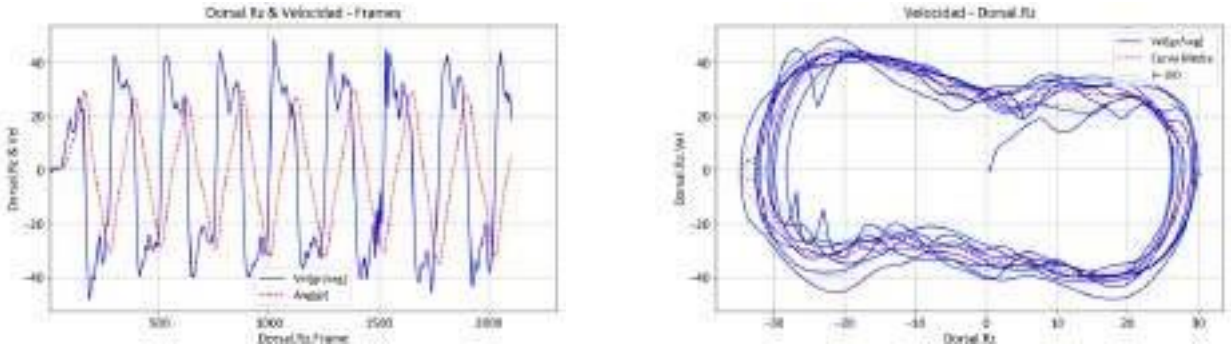

Fig 13. Gráficos Velocidad Angular

Units: Rot[gr/seg] Trans[cm/seg]

Columna.Lat	*Valor captura*	*Valores Referencia*	*Diferencia %*
Rz.Speed.Max	49.0	[39, 68, 97]	-28 % (en rango)
Rz.Speed.MaxMean	45.3	[35, 62, 89]	-27 % (en rango)
Rz.Speed.MaxStd	2.1	[0, 6, 12]	En rango
Rz.Speed.MaxCV[%]	4.6	[0, 8, 18]	En rango
Rz.Speed.Min	-48.0	[-37, -71, -104]	-32 % (en rango)
Rz.Speed.MinMean	-42.8	[-33, -64, -96]	-34 % (en rango)
Rz.Speed.MinStd	3.2	[0, 5, 10]	En rango
Rz.Speed.MinCV[%]	-7.5	[-1, -7, -13]	En rango
Rz.Speed.AreaMean	74.9	[48, 158, 267]	-52 % (en rango)
Rz.Speed.AreaStd	23.7	[0, 56, 113]	En rango
Rz.Speed.AreaCoef[%]	31.6	[7, 36, 66]	-12 % (en rango)

Dorsal.Rz.Speed.MaxPeaks[Val,Ang,fr]: [49.0, -21.0, 1023] [45.2, -27.1, 1532] [44.2, -20.3, 776] [44.2, -18.0, 2055] [44.0, -21.2, 1280]

Dorsal.Rz.Speed.MinPeaks[Val,Ang,fr]: [-48.0, 17.9, 181] [-43.4, 18.1, 1926] [-41.9, 14.5, 1681] [-40.7, 0.1, 1442] [-40.0, 17.4, 649]

6.3 Resultados: 03s1.Columna.Lat - Dorsal.Rz.SpeedUp

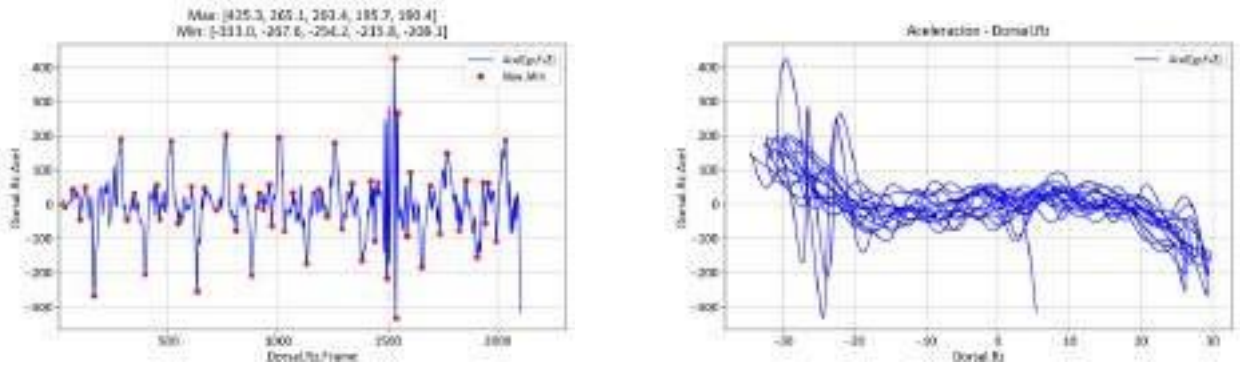

Fig 14. Gráfico Aceleración Angular

Units: Rot[gr/seg2] Trans[cm/seg2]

Columna.Lat	*Valor captura*	*Valores Referencia*	*Diferencia %*
Rz.SpeedUp.Max	425.3	[111, 286, 460]	49 % (ok)
Rz.SpeedUp.MaxMean	256.0	[90, 225, 360]	14 % (ok)
Rz.SpeedUp.MaxStd	99.3	[0, 46, 96]	A valorar
Rz.SpeedUp.MaxCV[%]	38.8	[0, 18, 40]	En rango
Rz.SpeedUp.Min	-332.98	[-33, -318, -603]	5 % (ok)
Rz.SpeedUp.MinMean	-255.7	[-59, -238, -416]	7 % (ok)
Rz.SpeedUp.MinStd	49.9	[0, 65, 143]	En rango
Rz.SpeedUp.MinCV[%]	-19.5	[0, -21, -47]	En rango
Rz.SpeedUp.Harmony	-0.6	[-0.35, -0.59, -0.82]	2 % (ok)
Rz.SpeedUp.Offset[deg]	126.5	[109, 126, 143]	0 % (ok)

Dorsal.Rz.SpeedUp.MaxPeaks[Val,Ang,fr]: [425.3, -29.6, 1529] [265.1, -22.0, 1542] [203.4, -29.5, 760] [195.7, -32.4, 1002] [190.4, -29.4, 282]

Dorsal.Rz.SpeedUp.MinPeaks[Val,Ang,fr]: [-333.0, -24.4, 1536] [-267.6, 29.3, 161] [-254.2, 26.1, 631] [-215.8, -23.8, 1495] [-208.1, 29.5, 878]